

Centre Armand Frappier Santé et Biotechnologie

Synthesis of a fluorinated library applied to fragment-based drug discovery via ^{19}F NMR with confirmed binding to HRAS-G12V

By

David Bendahan

A thesis presented in partial completion of the requirements for a
Masters in Science (M.Sc.)

Evaluation Committee

External examiner	Shawn Collins UdeM
Internal examiner	Annie Castonguay INRS-CAFSB
Research Director	Steven LaPlante INRS-CAFSB
Research Co-director	Pat Forgione Concordia University

ACKNOWLEDGEMENTS

Although all of the work presented is my own, it would be remiss of me not to acknowledge all of the help that I have received.

Even though it is unlikely that they will ever read this document, I must thank my parents for their support. Without a roof, warm meals and the affection that they have showed me, I would not be where I am today.

Dr. LaPlante, your go-get it attitude has been highly motivational and I thank you for all the support and guidance that you have provided.

Dr. Forgione, thank you for teaching me that in industry, a target is just a target and that there will always be more compounds to make. That really helped me get my priorities straight.

Dr. Woo, it was a privilege to work with you. I cannot thank you enough for the instruction and support that you have provided.

A tremendous amount of credit belongs to Yann Ayotte. I would like to thank him for the advice as well as all the tips that he taught me.

I would like to thank all the other lab members who have helped in no small way throughout my M. Sc.

Several members of the Forgione group need mentioning as well: Fadil Taç, Cindy Buonomano, Franklin Chacon Huete and Peter Liu; Thank you.

The members of my committee deserve my appreciation for taking time out of their (busy) schedules to read my thesis and listen to me babble on about my project.

To Nathalie, thank you for being an amazing partner and pushing me to complete this when all I wanted to do was give up.

RÉSUMÉ

Ici, une chimiothèque de fragments fluorés, bicycliques, à base de thiophène a été synthétisée de manière modulaire pour être utilisée en ^{19}F -RMN contre quelques protéines qui présentent un intérêt pour la communauté scientifique pour la découverte de futur médicaments. Pour certains composés de la bibliothèque synthétisée, la liaison a été détectée contre le mutant H-RAS (G12V), une cible notoirement difficile à cibler. La liaison a été détectée pour certains des analogues et ensuite suivie avec ^{15}N HSQC qui a confirmé la survenue d'un événement de liaison. Pour exclure la possibilité que la liaison soit promiscuité, le meilleur fragment de liaison a été criblé contre une protéine non reliée, la RNase 5 et n'avait aucune affinité. Ce projet est un excellent exemple de la vitesse et de la puissance de la découverte de médicaments à base de fragments, en particulier lorsqu'il est associé aux efforts de chimie synthétique interne. Les bibliothèques à base de fragments peuvent être synthétisée et testée en quelques jours via RMN.

Mots-clés : Découverte de médicaments basée sur des fragments, synthèse de chimiothèque, RMN du fluor, DLBS, HRAS-G12V

ABSTRACT

Herein, a fluorinated, bicyclic, thiophene based fragment library was synthesized in a modular fashion to be screened via ligand observed ^{19}F NMR against two proteins that are of interest to the scientific community. For certain compounds in the synthesized library, binding was detected against the H-RAS mutant (G12V) a notoriously undruggable target. Binding was detected for some of the analogs and subsequently followed up with ^{15}N HSQC that confirmed the occurrence of a binding event. To exclude the possibility that the ligand binding was promiscuous, the best binding fragment was screened against an unrelated protein, RNase 5 and was shown to exhibit no affinity. This project is a great example of the speed and power of fragment-based drug discovery especially when coupled with in-house synthetic chemistry efforts. Libraries can be synthesized then screened in days via ligand and protein observed ^1H and ^{19}F NMR.

Keywords : *Fragment-based drug discovery, library synthesis, Fluorine NMR, DLBS, HRAS-G12V*

SOMMAIRE RÉCAPITULATIF

Le domaine de la découverte de médicaments a involontairement commencé par l'observation des propriétés curatives de certaines plantes. Un exemple frappant est celui de la famille des salicylates que l'on trouve à l'état naturel dans le myrte et sur l'écorce du saule.¹ L'un des plus anciens textes médicaux conservés, le papyrus Ebers, décrit les propriétés analgésiques du myrte.² Hippocrate lui-même (célèbre pour son serment d'Hippocrate) a écrit sur les propriétés médicinales des copeaux d'écorce de saule.³ L'extraction de ces fleurs a donné des concentrés de produits naturels que l'humain applique à certaines maladies depuis des générations. La découverte des médicaments a évolué des produits naturels aux médicaments semi-synthétiques, comme l'Aspirine.

L'Aspirine, ou acide acétylsalicylique (structure **B** dans la Figure 1.1) est un exemple précoce de l'effort de chimie médicinale de la société Bayer pour améliorer la puissance d'un produit naturel en l'acétylant. L'acétylation est une réaction qui ajoute un groupe acétyle sur un oxygène ou un azote. Ce processus rend un composé plus lipophile, ce qui peut modifier considérablement ses propriétés pharmacocinétiques. La conversion d'un produit naturel en une autre substance (potentiellement) plus puissante produit ce que l'on appelle des médicaments semi-synthétiques et a été l'une des premières étapes de la progression de la découverte de médicaments vers ce qu'elle est devenue aujourd'hui.

Aujourd'hui, la découverte moderne de médicaments a considérablement progressé par rapport aux onguents dérivés de produits naturels du passé et comprend désormais des approches phénotypiques, génomiques et ciblées, ainsi que des variantes de l'approche semi-synthétique décrite ci-dessus. En général, les entreprises pharmaceutiques entament le plus souvent une campagne de découverte de médicaments par le criblage à haut débit (HTS) et la découverte de médicaments par fragments (FBDD).

La découverte de médicaments basée sur des fragments devient de plus en plus une alternative populaire à la HTS dans le domaine de la découverte de médicaments.⁹ Si la HTS peut être considérée comme une approche descendante, où un liant fort est détecté, décomposé en composants et reconstruit en un candidat clinique plus viable, la FBDD peut être qualifiée d'approche ascendante, par laquelle des molécules bioactives structurellement simples sont identifiées et construites en candidats cliniques puissants. La FBDD élimine la plupart des inconvénients de la HTS. Les fragments ont une structure moins complexe, ce qui permet de mieux sonder l'espace chimique et donc d'obtenir des résultats plus élevés.

Le nombre de composés potentiels contenant jusqu'à 11-16 atomes lourds (des fragments) est estimé à environ $10^7 \sim 10^9$ composés¹⁰⁻¹², ce qui représente une différence notable par rapport aux $\sim 10^{63}$ composés potentiels contenant jusqu'à 30 atomes lourds. Essentiellement, une bibliothèque de fragments de l'ordre d'un millier de composés couvre un échantillon beaucoup plus grand de l'espace chimique que les centaines de milliers à un million de composés présent dans une HTS.¹³ Un autre avantage d'avoir des fragments comme points de départ est la facilité de leur diversification synthétique. Moins il y a de groupes

fonctionnels sur un composé, plus il est facile de synthétiser des dérivés pour effectuer des relations structure-activité dans le but d'améliorer l'affinité. Lorsqu'il s'agit d'établir des relations structure-activité avec des fragments, des méthodes très sensibles sont nécessaires. Deux des technologies les plus courantes sont la RMN et la cristallographie. Ici, il est important de faire la différence entre l'efficacité du ligand et l'affinité de liaison. Les fragments plus petits auront une puissance plus faible que les composés de type HTS, car ils sont considérablement plus petits et ont globalement moins d'interactions. Cependant, les fragments de liaison ont tendance à avoir une efficacité de ligand plus élevée car il y a plus d'interactions qui se produisent par atome lourd.

La spectroscopie RMN peut être divisée en deux grands groupes. L'observation des protéines et l'observation des ligands, où le signal de la protéine ou du ligand est analysé respectivement. La plupart des techniques d'observation du ligand présentent des caractéristiques similaires. Elles utilisent des expériences unidimensionnelles relativement rapides au proton (^1H) ou au fluor (^{19}F), elles ne nécessitent pas de concentrations élevées de protéines et le marquage de la protéine avec des isotopes coûteux (^2H , ^{13}C ou ^{15}N) n'est généralement pas nécessaire. En outre, les techniques de RMN basées sur les ligands sont assez sensibles et sont idéales pour la détection de fragments à faible liaison. Ces caractéristiques rendent les techniques de RMN observées par ligand pratiques pour les phases initiales d'une campagne basée sur les fragments.

La technique unidimensionnelle la plus simple consiste à observer le spectre RMN (^1H ou ^{19}F) de l'échantillon de ligand libre en solution et de l'échantillon de ligand en présence de protéine pour voir s'il y a un changement dans le déplacement chimique (emplacement en ppm du signal) et/ou si le signal s'est élargi. Le décalage se produit parce que l'environnement chimique du liant est différent en présence d'une cible avec laquelle il interagit. L'élargissement se produit parce que, dans le cas de liants à faible interaction, l'échange entre l'état actif et l'état inactif est plus rapide que l'échelle de temps RMN²⁰ et le pic résultant est observé comme un pic large qui est un hybride du pic actif et du pic inactif.

Au lieu de se fier aux changements dans le spectre d'un fragment de liaison, on peut examiner les changements induits dans la protéine à la suite de la liaison. Cette approche fournit des détails supplémentaires qui sont précieux pour les chimistes médicaux, tels que la localisation du site de liaison et la constante de dissociation. Le ^{15}N -HSQC est de loin la technique la plus utilisée pour déterminer les changements de déplacement chimique dans une cible protéique d'intérêt.³³ Bien que cela ne soit pas strictement nécessaire, la protéine est uniformément marquée avec l'isotope ^{15}N afin de réduire le temps (coûteux) de RMN nécessaire à l'expérience. Le ^{15}N -HSQC est une expérience de corrélation bidimensionnelle qui fournit l'environnement chimique distinct de chaque liaison N-H présente sur la protéine. À l'exception de la proline, cela équivaut généralement à une par acide aminé, en raison des liaisons amides, mais certains signaux peuvent également provenir d'acides aminés contenant des chaînes latérales N-H (arginine, asparagine, glutamine, tryptophane) ou des domaines N-terminaux.

Malgré tout, par rapport à un HSQC ^1H - ^{13}C , les spectres HSQC ^{15}N sont beaucoup plus simples à interpréter et à produire.³³

L'objectif de ce projet était double. Le premier objectif était de synthétiser une bibliothèque de petites molécules et le second objectif était de cribler la bibliothèque synthétisée contre HRAS (G12V).

Une chimiothèque de fragments fluorés, bicycliques, à base de thiophène a été synthétisée de manière modulaire pour être utilisée en ^{19}F -RMN contre quelques protéines qui présentent un intérêt pour la communauté scientifique pour la découverte de futur médicaments. La GTPase HRAS est impliquée dans la régulation de la division cellulaire en réponse à la stimulation des facteurs de croissance. HRAS agit comme un interrupteur moléculaire marche/arrêt, une fois qu'il est activé, il recrute et active les protéines nécessaires à la propagation du signal du récepteur. HRAS se lie au GTP à l'état actif et possède une activité enzymatique qui coupe le phosphate terminal de ce nucléotide en le convertissant en GDP. En général, lors de la conversion du GTP en GDP, HRAS est désactivé, mais certaines mutations de HRAS, comme la mutation G12V, font que HRAS est activé en permanence, ce qui entraîne une croissance cellulaire incontrôlée et la formation d'une tumeur.

Le premier objectif était de synthétiser les différents fluorophényl thiophène amides et sulfonamides de manière modulaire et parallèle. Cette stratégie de construction modulaire simplifierait les cycles ultérieurs de synthèse d'analogues, s'ils s'avéraient nécessaires. L'approche modulaire permet de substituer facilement presque toutes les fonctionnalités des fragments d'intérêt. L'approche de synthèse parallèle a été adoptée pour réduire le temps nécessaire à la synthèse et à la purification des composants de la bibliothèque. En adaptant un protocole de la littérature³⁵, le noyau bicyclique a été construit en utilisant un couplage décarboxylatif catalysé par le palladium en utilisant le sel de potassium du 3-amino-thiophène-2-carboxylate qui a été synthétisé à partir de l'ester méthylique (schéma 1). Le couplage décarboxylatif au palladium présente plusieurs avantages par rapport aux réactions de couplage croisé plus classiques catalysées par le palladium. En commençant par les matériaux de départ, les composés contenant la fonctionnalité acide carboxylique ont tendance à être relativement peu coûteux, facilement disponibles et stables.³⁶ Deuxièmement, les couplages décarboxylatifs extrudent du dioxyde de carbone contrairement aux accouplements Stille ou Kumada qui extrudent des quantités stochiométriques de déchets métalliques tels que l'étain ou le magnésium.³⁷

Le centre bicyclique de la chimiothèque a été synthétisé via le couplage décarboxylatif catalysé par le palladium à partir de **(2)** qui lui a été préparé par la saponification de l'ester **(1)**. Les trois amines **(3)**, **(4)** et **(5)** qui ont été générées ont servi pour la synthèse des autres fragments de la chimiothèque **(6)** – **(29)**.

Les rendements pour le composé **(5)** étaient entre 56 et 71 %, tandis que les rendements pour le **(3)** atteignaient 82 %. Le suivi de la progression de la réaction par GC-MS a révélé que la quantité du produit secondaire homocoupleur indésirable (4,4'-difluoro-1,1'-biphényle) dans le cas de la réaction de couplage avec le fluor en position para au brome était plus élevée que dans le cas de la réaction de couplage ortho, ce qui explique le rendement réduit. Les composés **(3)**-**(5)** n'étant pas stables sous leur forme de base

libre, il a été nécessaire de former puis de stocker les composés sous forme de sels HCl. Par la suite, en utilisant l'amine comme poignée, les trois noyaux bicycliques ont été diversifiés en divers sulfonamides et amides (schéma 2). Cette chimie a été réalisée dans un format parallèle brut. Pour chacune des trois séries du schéma 2, 8 fioles séchées au four ont été étiquetées et rincées à l'azote avant l'addition de 1 mL de pyridine et de 50 mg du sel HCl des amines correspondantes **(3)**, **(4)** ou **(5)**. La dissolution (et donc la conversion en forme de base libre) a été instantanée. Les réactions avec les chlorures d'acide et les chlorures de sulfonyle étant assez exothermiques, les flacons ont tous été placés sur la glace avant l'addition de 1.2 équivalent du chlorure de sulfonyle ou d'acide correct à chaque réaction. La progression de la réaction a été suivie par CCM et, une fois la réaction terminée, le solvant a été concentré sous vide avant d'être purifié par chromatographie sur colonne flash en phase normale sans préparation, ce qui simplifie encore plus le processus. Les fragments ont été testés par RMN ^{19}F contre HRAS (G12V). Les signaux (Figure 3.4) bleues, dans les spectres ^{19}F , représentent le fluor libre (sans protéine) et les signaux rouges représentent l'environnement chimique du fluor en présence de protéine. Une différence dans les deux est une indication d'une affinité du ligand pour la protéine en question. Avec la plus grande divergence entre les spectres bleu et rouge, le fragment **(14)** a été déterminé comme ayant la plus grande affinité et donc le fragment **(14)** avait l'aire d'être le plus intéressant et a mérité d'être suivi par d'autres expériences. À l'aide de MOE, un logiciel de chimie computationnelle qui permet de visualiser les interactions composé-protéine, le fragment **(14)** et le fragment étroitement apparenté **(15)** ont été arrimés à HRAS (G12V). Les résultats de l'étude de docking sont présentés dans la figure 3.5. L'étude de docking indique que le groupe méthylène supplémentaire sur la fonctionnalité sulfonamide dans le composé **(15)** empêche l'entrée dans la poche peu profonde sur le HRAS (G12V) et par conséquent, une liaison hydrogène importante entre l'azote du sulfonamide et l'Asp 54 est empêchée. Ceci est en contraste avec le composé **(14)** qui, en raison de la plus petite taille du substituant, est capable de s'insérer dans la poche de la protéine et de former la liaison hydrogène entre l'Asp 54 et l'azote sulfonamide. Même si le composé **(14)** était plus exposé au solvant que le composé **(15)**, l'interaction de liaison hydrogène a contribué à elle seule à $-4,5$ kcal/mol à l'énergie de liaison globale. Ceci explique pourquoi le fragment **(15)** qui est structurellement très similaire au fragment **(14)** n'avait pas d'affinité pour HRAS (G12V).

Avant de s'engager dans un HSQC ^{15}N , il était impératif de déterminer la solubilité maximale des fragments de liaison. Nous avons souhaité confirmer la solubilité des meilleurs liants. La solubilité a été déterminée à l'aide d'un étalon externe d'acide maléique en utilisant la méthode ERETIC.⁵⁶ Les résultats de cette expérience sont illustrés dans la figure 3.6. Ils montrent que sur nos quatre liants détectés par RMN ^{19}F , trois composés **(14)**, **(17)** et **(25)** étaient assez solubles jusqu'à environ 2400, 1700 et 3800 μM respectivement et qu'un composé, **(20)**, n'était soluble que jusqu'à ~ 100 μM . Une solubilité élevée du ligand est très importante pour la détermination du K_d par HSQC ^{15}N . Le composé est généralement titré, et une faible solubilité ne fournirait pas de données adéquates pour obtenir la constante de dissociation.

Maintenant qu'il a été déterminé que le fragment **(14)** était soluble, nous voulions nous assurer que la liaison n'était pas promiscuité. Par conséquent, nous avons criblé le fragment **(14)** contre une protéine non apparentée, la RNase 5. L'absence de liaison est une indication que le fragment n'est pas promiscues. Avec cette information en main, nous avons procédé à l'expérience HSQC.

Après avoir confirmé la solubilité maximale de **(14)** et le faite que le fragment n'est pas promiscues, l'affinité du fragment **(14)** a été mesurée par 15N HSQC ¹⁵N et les résultats sont illustrés dans la figure 3.8. Plusieurs signaux représentant des résidus de protéines dans l'expérience HSQC se sont clairement déplacés et se trouvent donc dans un environnement chimique différent. Ceci est une autre indication que le fragment **(14)** se lie effectivement à HRAS (G12V).

En conclusion, l'objectif de ce projet était de synthétiser de façon modulaire une bibliothèque de fragments fluorés, bicycliques, basés sur le thiophène et de cribler la bibliothèque par RMN ¹⁹F contre deux protéines d'intérêt pour la communauté scientifique, HRAS et RNase 5. Quatre composés de la bibliothèque ont montré une affinité avec HRAS (G12V) par des méthodes d'observation du ligand. Pour confirmer la liaison à la cible, le fragment le plus puissant **(14)** a été suivi par une expérience ¹⁵N-HSQC avec HRAS (G12V) marqué au ¹⁵N. Dans la figure 3.8, il est évident que plusieurs résidus de HRAS ont un environnement chimique différent en présence du fragment **(14)**, ce qui est une indication claire de liaison. La promiscuité de liaison a été exclue par un contre-criblage du fragment avec une protéine non liée à HRAS, la RNase 5, qui a montré qu'aucune liaison ne se produisait.

Même si le fragment **(14)** présente une affinité de liaison pour HRAS (G12V), il est loin d'être un médicament et ne constitue qu'un point de départ. Par conséquent, les travaux futurs nécessiteront d'améliorer la puissance, la sélectivité et le profil pharmacocinétique du candidat. Plusieurs approches peuvent permettre d'améliorer la puissance. Une suggestion serait de cribler une plus grande bibliothèque de fragments en présence de HRAS (G12V) et du fragment **(14)** afin de trouver un second fragment qui a une affinité pour HRAS avec le fragment **(14)** en place. Si ce second fragment était trouvé, une structure cristalline de HRAS (G12V) en présence des deux fragments permettrait aux chimistes médicaux de lier potentiellement les fragments en fonction de la distance relative entre eux. Une autre option serait de faire croître successivement le fragment en ajoutant des substituants à diverses positions sur le noyau bicyclique afin d'améliorer l'affinité.

TABLE OF CONTENTS

ACKNOWLEDGEMENTS	2
RÉSUMÉ	3
ABSTRACT	4
SOMMAIRE RÉCAPITULATIF	5
TABLE OF CONTENTS	10
LIST OF FIGURES	11
INTRODUCTION: BACKGROUND ON DRUG DISCOVERY	12
1.1 MODERN DRUG DISCOVERY	13
1.1.1 <i>High Throughput Screening</i>	13
1.1.2 <i>Fragment-Based Drug Discovery</i>	15
1.2 NUCLEAR MAGNETIC RESONANCE	19
1.2.1 <i>Ligand Observed NMR Spectroscopy</i>	20
1.2.2 <i>Protein Observed NMR Spectroscopy</i>	22
2 STATEMENT OF THE PROBLEM	23
3 HYPOTHESES	24
4 MAIN OBJECTIVE AND SPECIFIC AIMS	25
5 DRAFT ARTICLE	26
6 DISCUSSION	33
6.1 LIBRARY SYNTHESIS	33
6.2 LIBRARY SCREENING	36
7 CONCLUSION AND PERSPECTIVES	44
8 REFERENCES	45
SUPPLEMENTAL INFORMATION	52

LIST OF FIGURES

FIGURE 1.1	ACETYLATION OF SALICYLIC ACID AND MORPHINE TO FORM SEMI-SYNTHETIC PRODRUGS.	12
FIGURE 1.2	GRAPHICAL DEPICTION OF THE HTS DRUG DISCOVERY PROCESS	14
FIGURE 1.3	THE CASCADE FROM HIGH-THROUGHPUT SCREEN TO A MARKETABLE DRUG	15
FIGURE 1.4	A VISUAL DESCRIPTION OF THE FRAGMENT-BASED APPROACH TO DRUG DISCOVERY	16
FIGURE 1.5	COMPARISON OF THE RELATIVE SIZE OF FRAGMENTS COMPARED TO FDA APPROVED DRUGS ..	17
FIGURE 1.6	FRAGMENT LINKING USED IN THE DISCOVERY OF A POTENT STROMELYSIN INHIBITOR.	18
FIGURE 1.7	THE DIFFERENT POTENCY ENHANCEMENT METHODOLOGIES APPLIED TO FRAGMENTS	18
FIGURE 1.8	DEPICTION OF THE ¹⁹ F- DLBS TECHNIQUE	21
FIGURE 1.9	ILLUSTRATION OF THE SLOW TO FAST EXCHANGE CONTINUUM	21
FIGURE 1.10	AN OVERLAY OF TWO ¹⁵ N-HSQC SPECTRA.....	22
FIGURE 3.1	GRAPHICAL ABSTRACT OF PROJECT.....	33
FIGURE 3.2	SELECTED EXAMPLES OF THIOPHENE CONTAINING DRUGS THAT WERE FDA APPROVED AND SUBSEQUENTLY HAD THEIR APPROVAL REVOKED DUE TO REACTIVE METABOLITE FORMATION...	36
FIGURE 3.3	COMPARISON OF OVERLAPPING PROTON AND FLUORINE NMR SPECTRA.....	38
FIGURE 3.4	¹⁹ F NMR LIGAND OBSERVED SCREENING RESULTS	39
FIGURE 3.5	DOCKING RESULTS FOR BEST BINDER (14) AND STRUCTURALLY SIMILAR NON-BINDER (15)	40
FIGURE 3.6	SOLUBILITY RESULTS FOR FOUR ¹⁹ F NMR DETECTED BINDERS	41
FIGURE 3.7	RESULT OF PROMISCUITY STUDY FOR COMPOUND 14. BINDING WAS NOT DETECTED VIA ¹⁹ F LIGAND OBSERVED NMR	42
FIGURE 3.8	HSQC SPECTRA OVERLAP OF HRAS (G12V) APO AND IN PRESENCE OF COMPOUND (14).....	42

INTRODUCTION: BACKGROUND ON DRUG DISCOVERY

The field of drug discovery unwittingly began with the observation that certain plants had curative properties. A prominent example is given by the family of salicylates that naturally occur in myrtle and on the bark of the willow trees.¹ One of the oldest surviving medical texts, the Ebers papyrus, describes the pain-relieving properties of myrtle.² Hippocrates himself (of Hippocratic Oath like fame) wrote about the medicinal properties of willow bark shavings.³ Extraction from these floras produced concentrates of natural products that humans have applied to certain ailments for generations.

Aspirin, or acetylsalicylic acid (**B**) was an early example of a medicinal chemistry effort by the Bayer Company to improve the potency of a natural product by acetylating it. Ironically, Felix Hoffmann, the man responsible for saving countless lives by acetylating salicylic acid to make Aspirin, is also responsible for developing heroin (**D**) by using the same acetylation technique he used on salicylic acid (**A**) applied to morphine (**C**).³ Although, most probably unbeknownst to him at the time, Dr. Hoffmann created prodrugs.

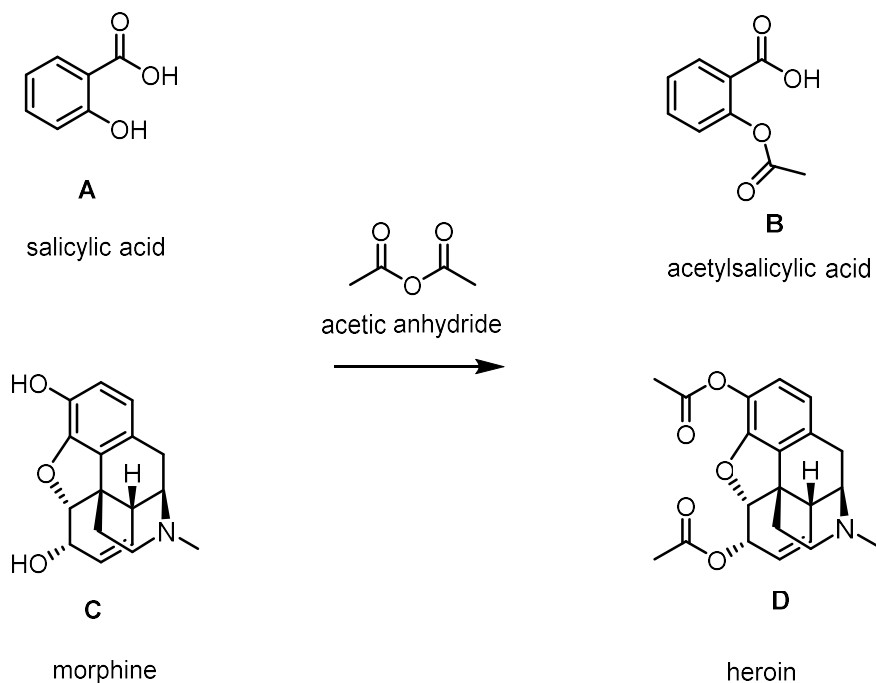


Figure 1.1 Acetylation of salicylic acid and morphine to form semi-synthetic prodrugs

Illustration showing the similarity between the conversion of the natural products, salicylic acid and morphine to Aspirin and heroin respectively. Both developed by the same chemist working for Bayer at the end of the 19th century, Felix Hoffmann and both act as prodrugs via in-vivo deacetylation by endogenous esterases

A prodrug is an inactive form of a drug that is activated *in-vivo*. For example, when ingested orally, the vast majority of heroin is processed by the liver to form morphine in what is known as the first pass metabolism. In healthy test subjects, one study⁴ determined that only 0.1% of the oral dose was excreted through urine in the acetylated form. On the other hand, when heroin was administered intravenously, thereby bypassing the first pass metabolism, roughly 70% of the excreted dose was present, untouched, in the diacetylated form. Acetylation of hydroxyl groups makes a compound more lipophilic (more attracted to fat than water). In the case of heroin, this is evidenced by a much higher partition coefficient. The partition coefficient is a ratio representing the relative concentration of a compound in a biphasic mixture of 1-octanol and water and is a rough representation of how the compound will be partitioned in the human body. For heroin the partition coefficient is 52 and when it is compared to the partition coefficient of morphine, which is 6, it is clear that the acetylation made the semi-synthetic heroin considerably more lipophilic than the naturally derived precursor, morphine.⁵ The higher the partition coefficient, the more fat soluble (or lipophilic) the compound. In the case of heroin, the dramatically increased lipophilicity brought on by the diacetylation allows it to freely pass the blood brain barrier (BBB) where it is then deacetylated to the active μ -opioid receptor agonist, morphine.⁵ With an IC_{50} of 483 nM,⁶ the binding affinity of heroin is roughly 10 fold less than that of morphine but the increased lipophilicity of the prodrug permits a higher peak concentration of morphine in the brain and is the explanation as to why heroin is more potent than morphine.

The process of converting a natural product into another (potentially) more potent substance produces what are known as semi-synthetic drugs and was one of the first steps in the progression of drug discovery to what it has become today.

1.1 Modern Drug Discovery

Modern drug discovery has dramatically advanced from the natural product derived ointments of the past and has gone on to include phenotypic, genomic and target-based approaches as well as variations of the semisynthetic approach described above. Because of the vastness of the field, this section of the text will focus on small molecule target-based approaches, most prominently high-throughput screening (HTS) and fragment-based drug discovery (FBDD).

1.1.1 High Throughput Screening

High throughput screening is the rapid testing of thousands to millions of compounds for biological activity, typically through the use of biochemical assays and automation. It is the most common way that major pharmaceutical companies begin a new drug discovery campaign. The chemical matter present in a high throughput screening library are typically complex drug like compounds with molecular weights

ranging from 300-500+ Daltons. The hits provided from a typical high throughput screen provide compounds with a binding affinity in the micromolar range. Subsequently, attempts to improve the pharmacodynamics (the effects and mechanism of action), pharmacokinetics (absorption, distribution, metabolism and excretion) and potency of the compound begin. Figure 1.2 provides an illustration of the process of drug discovery starting from a high throughput screen through to lead optimization.

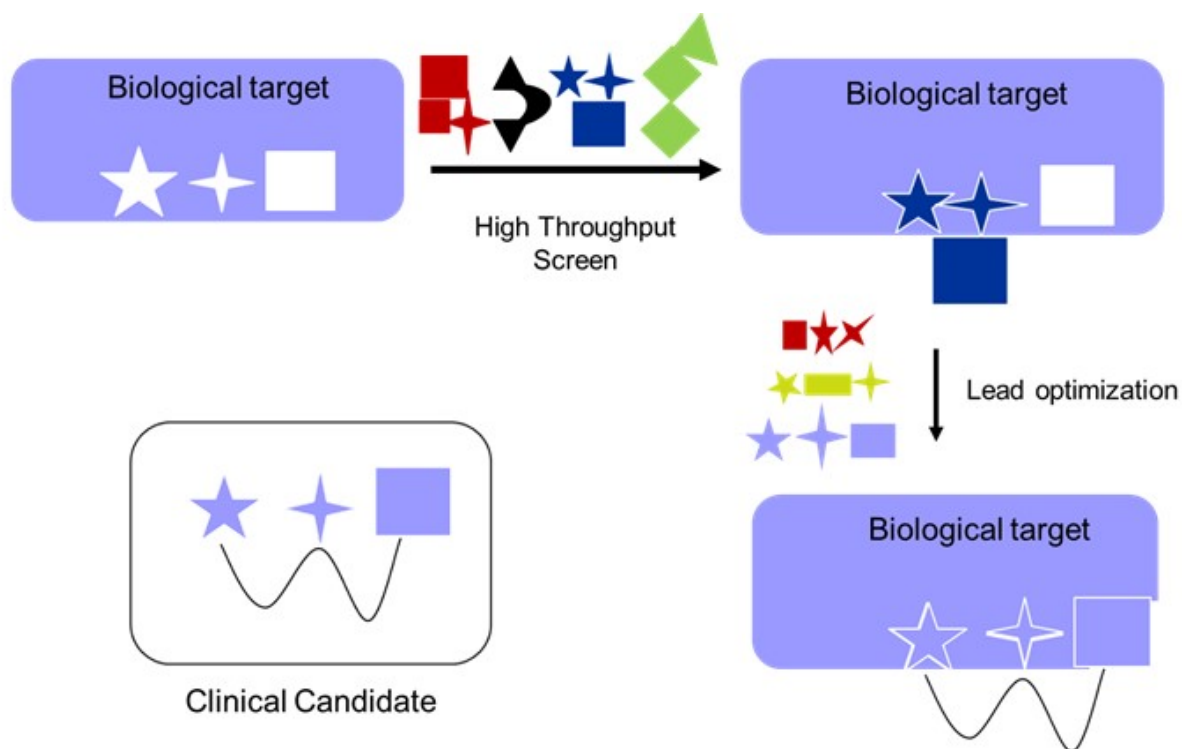


Figure 1.2 Graphical depiction of the HTS drug discovery process.

In a typical HTS, hundreds of thousands of compounds are screened to identify potentially useful chemical matter (depicted in dark blue) that interacts with the target. Subsequently, in the lead optimization phase, the compound is broken down and rebuilt, in order to make it a more potent and specific binder.

As was illustrated in figure 1.2, the hits that are provided from a typical HTS are not perfect binders because the compounds in the HTS library were not optimized for the target of interest and are structurally quite complex. Furthermore, one estimate⁷ pegs the number of potentially biologically active chemicals to be somewhere on the order of 10^{63} (assuming a maximum of 30 heavy atoms and restricting these heavy atoms to carbon, nitrogen, oxygen and sulfur). The entirety of all the libraries of compounds synthesized from every pharmaceutical company and academic lab to date is on the order of hundreds of millions⁸ for arguments sake let us assume that there are one billion (10^9) qualifying, different, small molecules in existence. If one were to run a high throughput screen with these one billion molecules, it would cost an exorbitant amount of time, money and manpower. Furthermore, the screen would not even cover one trillionth of one percent of chemical space. The main reason for this limitation is that the bigger the

compounds that are being screened, the higher the chances of it having a functional group or 3D motif that hinders binding. And so, because of the complexity of the HTS library components, the chances of finding a hit are quite small, typically 1-2 %.⁸ Furthermore, the active compounds are quite difficult to optimize whilst simultaneously maintaining the drug like properties required (detailed in section 1.1.2). As a result of the complexity, active compounds from a HTS must be broken down and rebuilt in order to have optimized physicochemical properties. So why not skip a step and just start from smaller compounds? That is the concept behind fragment-based drug discovery.

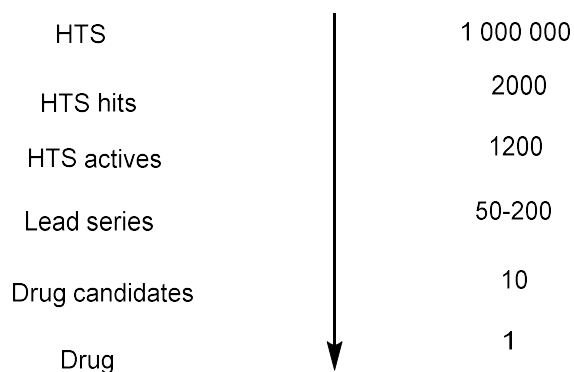


Figure 1.3 The cascade from high-throughput screen to a marketable drug

A figure illustrating the inefficiency of a high-throughput screen. Because of the complexity of the compounds contained in the HTS library, the screen needs to begin with a large number of compounds (~1 000 000) in order to be successful in coming up with some lead series. Adapted with permission from ref. [8] Copyright 2004 Elsevier.

All of the arguments above indicate that high-throughput screening is an inefficient and expensive endeavour that is only available to big, well-funded pharmaceutical companies and academic research groups, however, it is a tried and true method of drug discovery.

1.1.2 Fragment-Based Drug Discovery

Fragment based drug discovery (FBDD) is increasingly becoming a popular alternative to HTS in the field of drug discovery.⁹ If HTS can be considered as a top-down approach, where a strong binder is detected, broken down into components and rebuilt into a more viable clinical candidate, FBDD can be labelled a bottom-up approach whereby structurally simple bioactive molecules are identified and built into potent clinical candidates. FBDD eliminates most of the drawbacks present in HTS. The fragments are less structurally complex leading to better probing of chemical space and thus higher hit rates. The number of potential compounds that contains up to 11-16 heavy atoms is estimated to be roughly $10^7 \sim 10^9$ compounds,¹⁰⁻¹² a marked difference from the estimated $\sim 10^{63}$ potential compounds that contain up to 30 heavy atoms. Essentially, a fragment library on the order of a thousand compounds covers a dramatically bigger sample of chemical space than the hundred of thousands to a million compounds screened via HTS.¹³

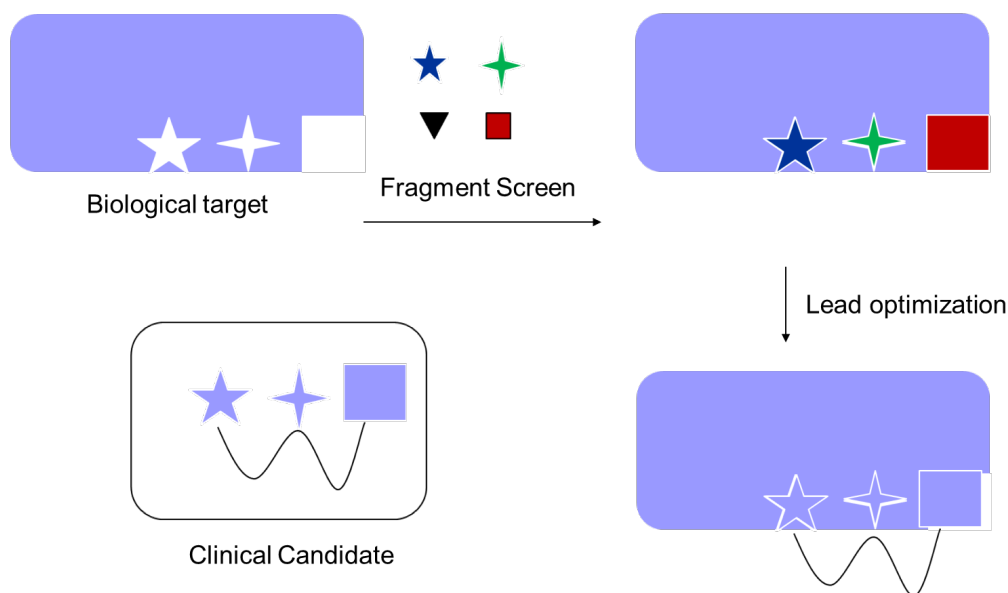


Figure 1.4 A visual description of the fragment-based approach to drug discovery

Fragment based drug discovery is a bottom-up approach that identifies weak, highly ligand efficient compounds that are grown, linked or merged into more potent compounds.

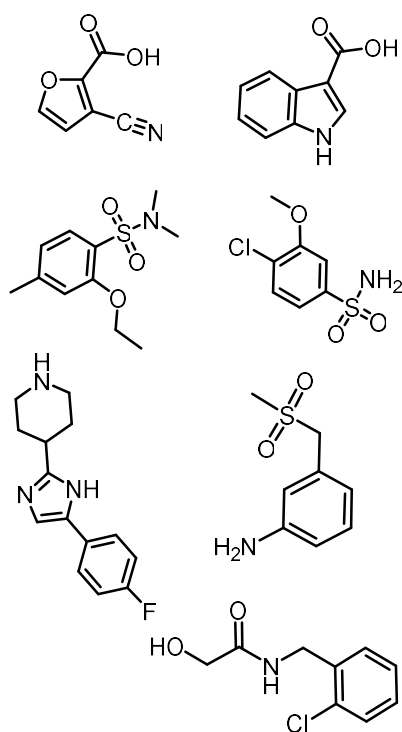
Another advantage of having fragments as starting points is the ease of their synthetic diversification. The less functional groups that are present on a compound, the easier it is to synthesize derivatives to perform structure activity relationships (SAR) in an attempt to improve the affinity.

Lipinski *et al.* from Pfizer came up¹⁴ with a guideline for the structural properties of drugs known as the rule of 5. Veber *et al.* improved¹⁵ this by including the concepts of limited rotatable bonds (to reduce the entropic cost of binding) and polar surface area, observations known to enhance oral bioavailability. As might have been grasped by now, fragments are smaller and structurally less complex than typical drug molecules; therefore, an adaptation of these guidelines was created¹⁶ for fragments by Congreve *et al.* at Astex and was dubbed the rule of 3. Table 1.1 is a side-by-side comparison of the different guidelines for drugs and fragments. Figure 1.5 has a selection of random fragments and drugs for size comparison. It should be noted that Lipitor, one of the best-selling drugs of all time¹⁷ does not respect most of the rules outlined in Table 1.1 and illustrates how the pharmaceutical industry uses these as guidelines and not as hard-truths that must be respected in every case.

Table 1.1: A side-by-side comparison of Lipinski's rule of 5 and Astex's rule of 3

Lipinski's Rule of 5 ¹⁴	Veber's modifications ¹⁵	Astex Rule of 3 ¹⁶
<ul style="list-style-type: none"> No more than 5 hydrogen bond donors No more than 10 hydrogen bond acceptors A molecular weight of less than 500 daltons A partition coefficient below 5 	<ul style="list-style-type: none"> Questioned the 500 dalton cutoff Added the concept of 10 or fewer rotatable bonds A polar surface area of less than 140 Å² 	<ul style="list-style-type: none"> No more than 3 hydrogen bond donors No more than 3 hydrogen bond acceptors Molar mass below 300 daltons No more than 3 rotatable bonds

Sample Fragments



Sample FDA approved drugs

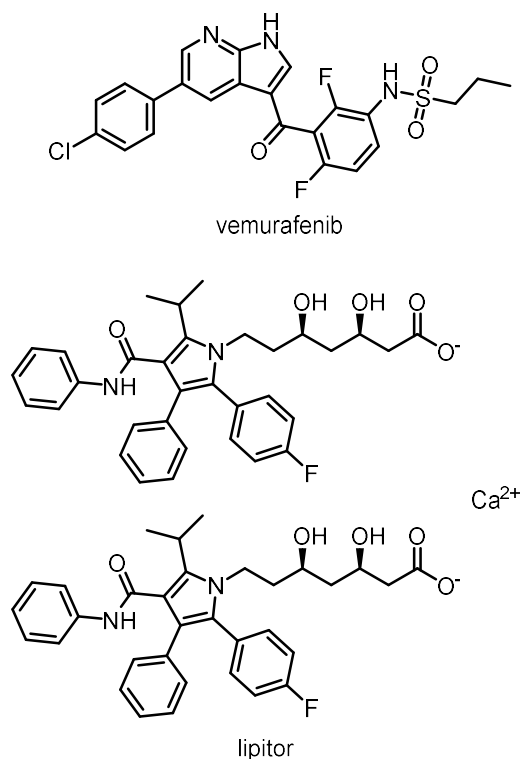


Figure 1.5 Side by side comparison of the relative size of fragments compared to FDA approved drugs

On the left, the sample fragments generally respect the rule of three outlined by Astex. Above, on the right, is Vemurafenib, A B-Raf enzyme inhibitor, was developed using FBDD.¹⁸ Bottom right is Lipitor, one of the best-selling drugs of all time.¹⁷ Note that Lipitor does not respect most of the guidelines outlined for drugs.

There are three major ways that fragments can be advanced into more potent lead like compounds. The fragment can either be merged, linked or grown. Merging fragments involves identifying fragments that bind in different parts of the same pocket of the target and combining them to improve affinity. Fragments in adjacent pockets can be linked to produce an exponentially more potent drug than the sum of the parts. For example, the paper¹⁹ that pioneered SAR by NMR and arguably brought FBDD

to the forefront of drug discovery research showed how the linking of two weakly binding ligands to an enzyme, stromelysin, produced a 15 nM inhibitor in less than 6 months.

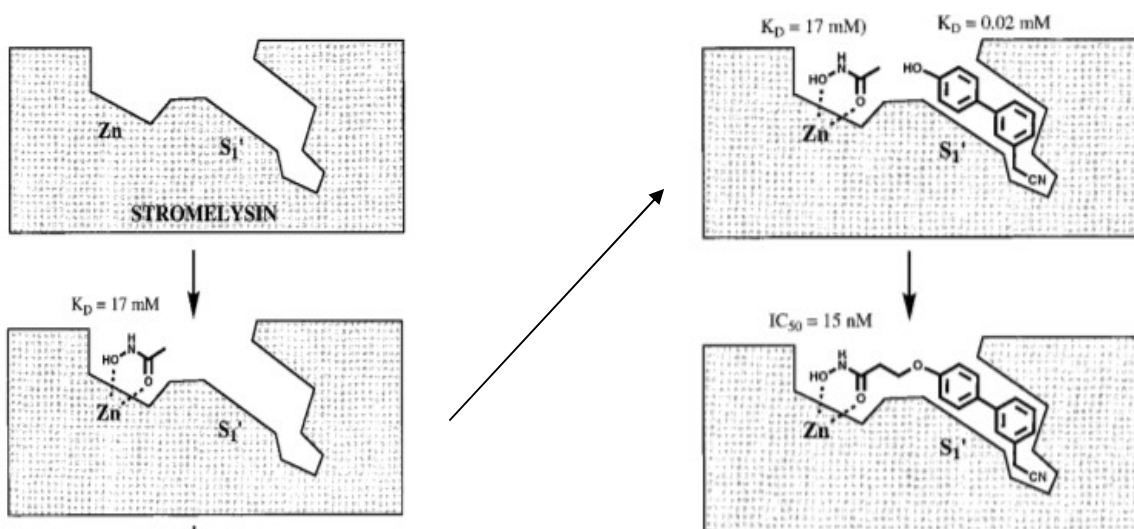


Figure 1.6 Fragment linking technique used in the discovery of a potent stromelysin inhibitor.

Two weakly binding fragments (17 mM and 0.02 mM) were discovered and subsequently linked to provide a 15 nM inhibitor. Adapted with permission from ref. [19] Copyright 1997 American Chemical Society.

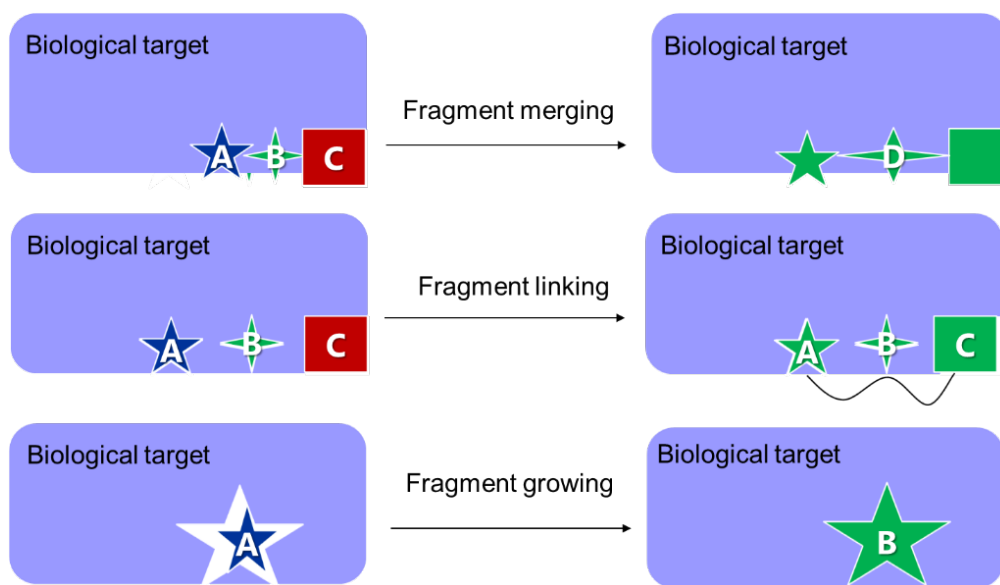


Figure 1.7: A depiction of the different potency enhancement methodologies applied to fragments.

Fragments can be merged whereby several fragments that were determined to be binding nearby in the same pocket can be merged into one. Fragments in different pockets can also be linked. A fragment can also be grown to produce a compound that would better fit the pocket (and provide better affinity)

The compounds present in a fragment library tend to be very weak binders but, in contrast, they are highly ligand efficient (they possess a high binding affinity per heavy atom). Their weak affinity (typically high μM to low mM) is due to their small size and limited functionalities that may interact with the target. This leads

to a drawback in FBDD in that the activity is generally not detectable at the biochemical screening concentrations used in a typical HTS as a result, more sensitive detection methods are required.

1.2 Nuclear Magnetic Resonance

Several biophysical methods such as surface plasmon resonance,²⁰ isothermal titration calorimetry,²¹ microscale thermophoresis,²² are sensitive enough to be used for detecting fragments that interact with a biochemical target of interest. They are useful as initial screening technologies but they do not provide structural information regarding the binding site. Due to their ability to provide structural insight as opposed to a yes or no answer, two technologies, X-ray crystallography²³ and nuclear magnetic resonance (NMR) spectroscopy,²⁴ have risen to the forefront of FBDD. A thorough report covering all these technologies would span several books, therefore, the focus of the following sections is on different NMR techniques that are applied to drug discovery. One major advantage that NMR spectroscopy inherently possesses over x-ray crystallography is the ability to study the binding interactions *in solution*.

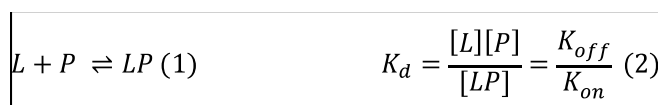
In the mid 20th century, several Nobel Prizes were awarded to the pioneers of NMR spectroscopy. The 1944 Nobel prize in physics went to Isidor Isaac Rabi,²⁵ who described and recorded the first nuclear magnetic resonance effect.²⁶ The 1952 Nobel prize in physics was awarded to Felix Bloch and Edward Mills Purcell “for their development of new methods for nuclear magnetic precision measurements...”²⁷ Nowadays, NMR has become one of the most routine technologies that allows for structural elucidation applied to the identification of small molecules.

If an isotope of a certain element has an even number of neutrons and protons, its angular momentum is zero, essentially its (quantum) total spin is said to be zero. If, on the other hand, there is an odd number of subatomic particles in the nucleus then the isotope is said to have a nonzero spin (due to its angular momentum) and possess a nuclear magnetic moment. In the presence of a strong magnetic field, the vast majority of the nuclear magnetic moments of the sample will be aligned in the direction of the magnetic field. Application of a magnetic field perpendicular to the original field will induce a precession (spinning of the nuclei in the sample) into the xy plane. The precession of each nucleus occurs at characteristic rates that depend on the chemical environment of the nucleus in question.^{28,29} NMR spectroscopy is the technology that exploits these **Nuclear Magnetic Resonances**. Isotopes such as ¹H, ¹³C, ¹⁵N, ¹⁹F, ³¹P and other odd numbered isotopes may be directly observed in an NMR spectrum. The relative position on the spectrum is related to the precession rate that in turn is dependent on the chemical environment of the atom in question. The chemical environment can be expressed as ν in Hertz (1/s), ω in (rad/s) but it is not useful for comparing results from spectrometers with different magnetic field strengths so the chemical environment is generally normalized to the field strength and represented in ppm (parts per million).²⁹ The chemical environment is affected mainly by the local environment of the nucleus in question (the effects of other nuclei present in the sample) but it is also affected by solvent, aromatic ring currents, charged species in solution, hydrogen bonding and bond torsion angles.³⁰ If a ligand interacts with a protein, the

local environment for the nuclei that constitute the ligand and the protein would be different than if either one was free in solution.³⁰

The different NMR techniques applied to drug discovery can be broadly split into two families. When the binding is detected by observing the signals belonging to the ligand it is a technique that falls under the guise of ligand observed NMR spectroscopy and if the signals originating from the protein are being used as the detection method, the technique falls under the protein observed NMR spectroscopy family.³¹

Medicinal chemists generally look for binders that interact noncovalently. This leads to the binding of a ligand to a target protein to generally be an equilibrium between the ligand binding (on) and the ligand detaching (off). This phenomenon is described by the dissociation constant (K_d). The dissociation constant is also correlated to the rate of binding (K_{on}) and rate of detachment (K_{off}).³²



- (1) Describes the formation of the ligand protein complex (LP) from the binding of the ligand (L) to the protein (P)
- (2) Defines the relationship between the dissociation constant where [L] is the ligand concentration [P] is the target protein concentration and [LP] is the concentration of the protein ligand complex.

1.2.1 Ligand Observed NMR Spectroscopy

Most ligand observed techniques have some similar characteristics. They use relatively quick one-dimensional proton (^1H) or fluorine (^{19}F) experiments, they do not require high concentrations of protein and labelling the protein with expensive isotopes (^2H , ^{13}C or ^{15}N) is not generally required. Furthermore, ligand-based NMR techniques are quite sensitive and are ideal for detection of weakly binding fragments. These characteristics make ligand observed NMR techniques practical for the initial phases of a fragment-based campaign.

The simplest one-dimensional technique is accomplished by observing the NMR spectrum (^1H or ^{19}F) of the ligand sample free in solution and the ligand sample in the presence of protein to see if there is a change in the chemical shift (location in ppm of the signal) and/or if the signal has broadened. Shifting occurs because the chemical environment of the binder is different in the presence of a target that it interacts with. Broadening occurs because, in the case of weakly interacting binders, the exchange between the on and off state are faster than the NMR timescale²⁰ and the resulting peak is observed as a broad peak that is a hybrid of the on peak and the off peak.

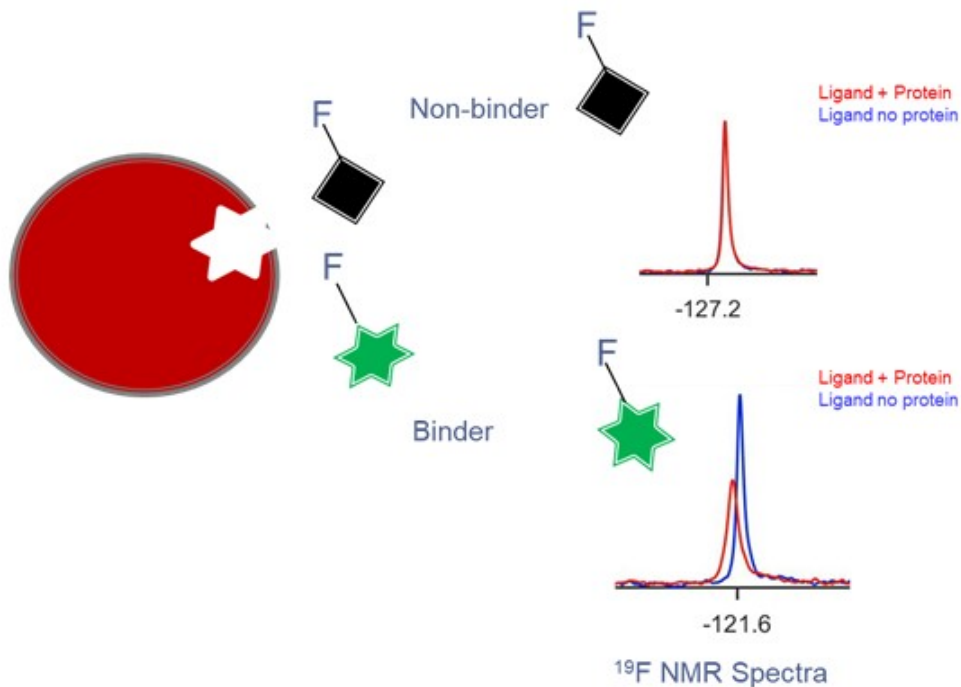


Figure 1.8: Depiction of the ^{19}F - DLBS technique

The ^{19}F NMR spectrum of a non-binder (black square) appears identical in the presence (red) and absence (blue) of protein (red oval). The ^{19}F NMR signal of a binder (green star) broadens and/or shifts as a result of the different chemical environment sensed by the fluorine isotope attached to the fragment.

There is a continuum ranging from slow exchange to fast exchange which is indirectly related to the K_d .

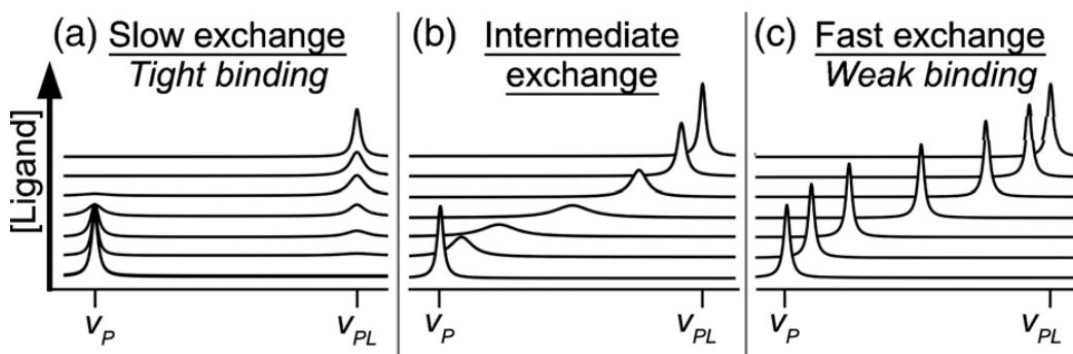


Figure 1.9: illustration of the slow to fast exchange continuum

Three typical 1-D NMR titrations: A tighter binder leads to scenario (a), slow exchange, the protein–ligand complex is long-lived and rarely dissociates during the timescale of the detection period of the NMR experiment. Intermediate exchange results in scenario (b) intermediate binding due to interconversion between the free and bound states during the detection period of the NMR experiment. Scenario (c) Fast exchange results from weak binding and rapid interconversion (thus averaging) during the detection period of the experiment taken from ref [30] with permission. Copyright 2010 Elsevier.

1.2.2 Protein Observed NMR Spectroscopy

Instead of relying on changes in the spectrum of a binding fragment, one can look at the changes induced to the protein as a result of the binding. This approach provides additional details that are valuable to medicinal chemists, such as binding site location and dissociation constant. ^{15}N HSQC is by far the most common technique used for determining the chemical shift changes in a protein target of interest.³³ Although not strictly necessary, the protein is uniformly labelled with the ^{15}N isotope in order to reduce the amount of (costly) NMR time required for the experiment. The ^{15}N -HSQC is a two-dimensional correlation experiment that provides the distinct chemical environment of every N-H bond present on the protein. Excluding proline, this typically equates to one per amino acid, due to the amide linkages, but some signals can also be a result of amino acids containing N-H side chains (arginine, asparagine, glutamine, tryptophan) or the N terminal domains. Even so, when compared to a ^1H - ^{13}C HSQC, ^{15}N HSQC spectra are dramatically simpler to interpret and produce.³³

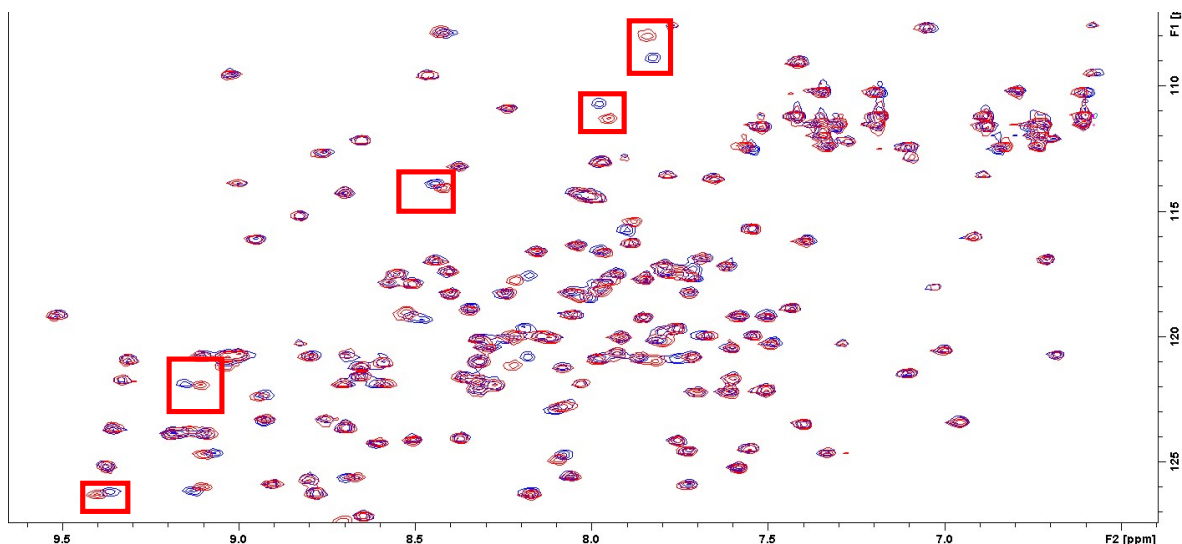


Figure 1.10 An overlay of two ^{15}N -HSQC spectra

The blue spectrum is an example of a 2D ^{15}N -HSQC of a protein in buffer. The red spectrum is the ^{15}N -HSQC spectrum of a protein in the presence of a binder. As can be seen, certain resonances are shifted as a result of binding. (^{15}N resonances on the y axis, ^1H resonances on the x axis)

Each of the points (resonances) on Figure 1.10 represents the N-H bond of a specific amino acid residue on the protein under observation. It is clear that the presence of a binder has changed the chemical environment of certain amino acids a lot more than others and some have not shifted at all. This is typically due to direct interactions between the ligand and the select protein residues³⁴ but it can also be due to allosteric effects brought on by conformational changes due to binding. If the residues have been assigned then it is possible to know the location of the binding site but the assignments are not necessary for determining the K_d .

2 STATEMENT OF THE PROBLEM

It is common knowledge in the oncology research community that RAS mutations are responsible for several types of cancers. Of the three proto-oncogenic isoforms, KRAS mutations are the most prominent in cancers, followed by NRAS and then HRAS. Because HRAS was the least important out of the three in terms of patient population, it was neglected as a drug target and the focus of the pharmaceutical community was on KRAS. Nonetheless, 5% of head and neck squamous cell carcinomas and 6% of bladder cancers originate as a result of HRAS mutations.^{57,58}

For many decades, HRAS has been considered an undruggable target⁵⁷ and no drug candidate has ever made it to market. Therefore, there is an unmet medical need to develop an HRAS inhibitor which could help to prolong the lives of many cancer patients.

3 HYPOTHESES

Since HRAS is known to be a difficult protein to target via the traditional high throughput screening approach, we hypothesized that a fragment-based approach may allow the discovery of new chemical matter that can interact with HRAS on a molecular level. Furthermore, since thiophenes are vastly under represented in drug candidates, it was hypothesized that screening a thiophene library against HRAS may lead to a starting point for a future drug discovery campaign.

4 MAIN OBJECTIVE AND SPECIFIC AIMS

The goal of this project was to set-up a starting point for future drug discovery campaigns that seek to develop a selective HRAS (G12V) inhibitor. In order to achieve this, the aims were twofold. The first was to synthesize a library of thiophene-based fragments because of their underrepresentation in most chemical matter libraries. The second aim was to use ^{19}F NMR to screen the synthesized fragments to determine if any had a binding affinity for HRAS (G12V).

Synthesis of a fluorinated library applied to fragment-based drug discovery via ^{19}F NMR with confirmed binding to HRAS-G12V

Synthèse d'une bibliothèque fluorée appliquée à la découverte de médicaments à base de fragments par RMN ^{19}F avec liaison confirmée à HRAS-G12V

Auteurs :

David Bendahan, INRS

Pat Forgione, Concordia University

Steven R. LaPlante, INRS

Titre de la revue ou de l'ouvrage : Bioorganic & Medicinal Chemistry Letters (not yet submitted)

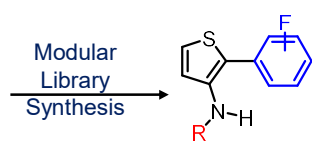
Graphical Abstract

Synthesis of a fluorinated library applied to fragment-based drug discovery via ^{19}F NMR with confirmed binding to HRAS-G12V

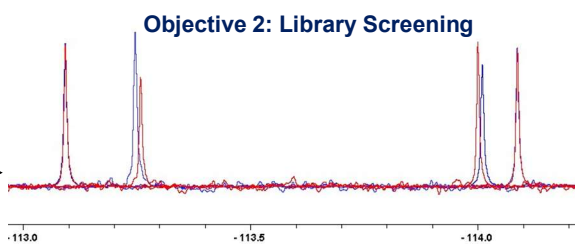
Leave this area blank for abstract info.

David Bendahan,^{a,b,c} Pat Forgione,^b Steven R. LaPlante^{a*}

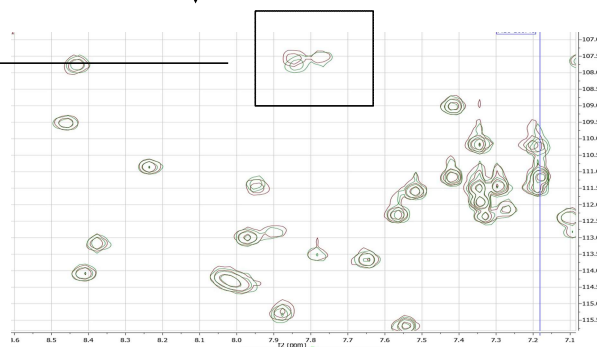
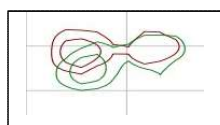
Objective 1: Library Synthesis



Screen by ligand observed ^{19}F NMR To detect binding



Confirm binding by ^{15}N HSQC



Synthesis of a fluorinated library applied to fragment-based drug discovery via ^{19}F NMR with confirmed binding to mutant HRAS-G12V

David Bendahan^{a,b,c}, Pat Forgione^b, Steven R. LaPlante^{a*}

^a INRS Centre Armand Frappier Santé et Biotechnologie, 531, boulevard des Prairies, Laval, Québec H7V 1B7, Canada

^b Department of Chemistry & Biochemistry, Concordia University, 7141 rue Sherbrooke O., Montréal, QC, Canada H4B 1R6

^c NMx Research and Solutions Inc., 500 Cartier Blvd. W., Suite 6000, Laval, Québec, Canada H7V 5B7

ARTICLE INFO

Article history:

Received

Revised

Accepted

Available online

Keywords:

Fragment-based drug discovery

Fluorine NMR

DLBS

library synthesis

HRAS-G12V

ABSTRACT

Herein, a fluorinated, bicyclic, thiophene based fragment library was synthesized in a modular fashion to be screened via ligand observed ^{19}F NMR against two proteins that are of interest to our group. For certain compounds in the synthesized library, binding was detected against the H-RAS mutant (G12V) a notoriously undruggable target. Binding was detected for some of the analogs and subsequently followed up with ^{15}N HSQC which confirmed the occurrence of a binding event. To exclude the possibility that the binding was promiscuous, the best binding fragment was screened against an unrelated protein, RNase 5 and was shown to be a non-binder. Additionally, a hypothesis provided by docking explains why a very similar compound to the best binder did not bind to HRAS (G12V).

2022 Elsevier Ltd. All rights reserved.

Time and time again, fluorine has proved to be an extremely valuable tool in both medicinal chemistry and drug discovery. Sterically speaking, the fluorine atom is not much larger than a hydrogen atom, not considering other isotopes of hydrogen, fluorine is the smallest substituent that can be used to replace a proton.¹ In particular, fluorine-19 (^{19}F) has been widely used as a probe of biological systems especially in the field of nuclear magnetic resonance (NMR).^{2,3} The ^{19}F nucleus is 100 % naturally abundant and has a high gyromagnetic ratio (~94 % that of hydrogen).⁴ In-vivo it can provide high quality images of live biological tissue using ^{19}F -MRI.^{5,6} In vitro, a plethora of different NMR techniques can be used by incorporating a fluorine on a macromolecular target or on the ligand itself.⁷⁻⁹ Perturbations in the fluorine NMR spectra of a ligand can be an indication of binding^{4,10} and is easily observed by comparing the NMR spectra of a ligand in the presence and absence of a protein target. (Figure 1). These changes in the NMR spectrum (broadening and chemical shift perturbation) are due to the quick exchange between the bound and unbound states. Because it happens so fast, the NMR sees an average of the on and off state hence the broadening and shifting.

Binding confirmation can be achieved by myriad other techniques. One particularly useful NMR technique used for binding confirmation is ^{15}N -HSQC. The main reason as to the popularity of this technique lies in the ability to provide structural information on which residues are affected by the ligand (allosterically or otherwise). Combined with the identity of each

cross-peak, ^{15}N -HSQC can be a very powerful tool in drug discovery.

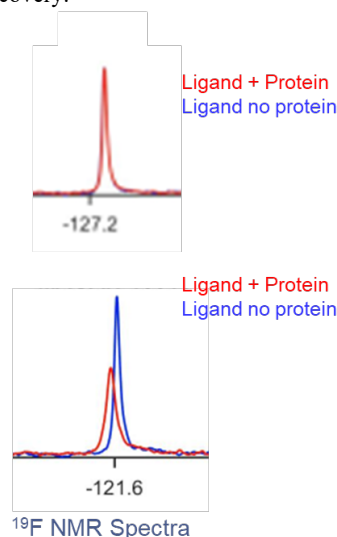
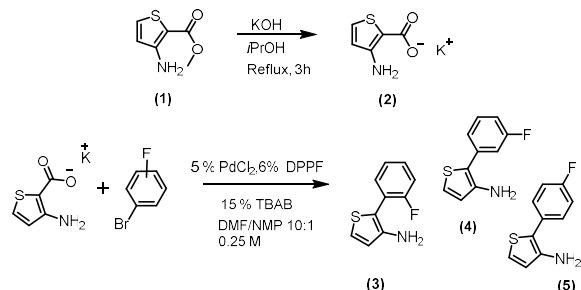


Figure 1: fluorine-19 DLBS experiment

The synthesis of the fluorinated bicyclic thiophene core was initiated by the saponification of methyl-3-aminothiophene-2-carboxylate (**1**) to provide potassium 3-aminothiophene-2-carboxylate (**2**). An adaptation of previously described⁸ palladium catalyzed decarboxylative cross-coupling using the corresponding *ortho*, *meta* or *para*-bromo fluorobenzene allowed us to obtain the bicyclic thiophene core with decent yields at gram scale (**Scheme 1**).



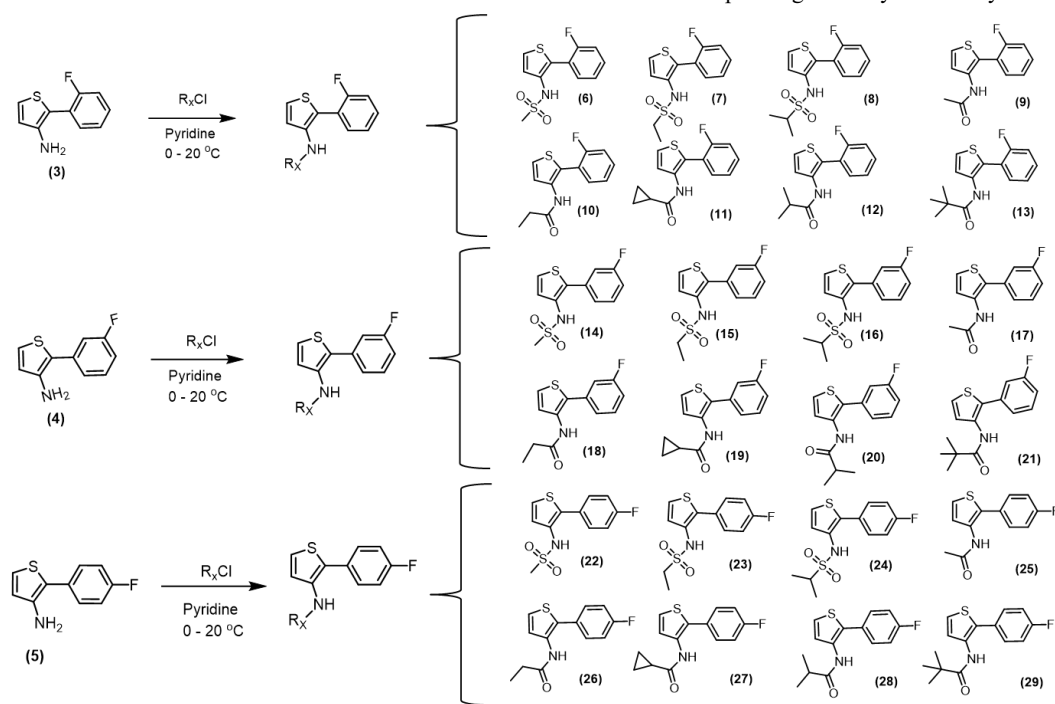
Scheme 1: Synthesis of the bicyclic core

To our knowledge and at the time of writing, there were no reports of these substrates having been synthesized previously. Initially, the yield of compound (**5**) was dramatically lower than the yields obtained for compounds (**3**) and (**4**). This was noted to be because of the increased formation of the *para* homocoupling side product. Dropwise addition of 1-bromo-4-fluorobenzene (

Although binders were detected for some members of the *para* family of analogs (**figure 3**) others were categorized as aggregators (**25**) and (**27**) and so more screening of the *para* analogs was not pursued in order to prevent potential false positives in downstream biochemical assays.^{11,12}

The screening of the *meta* family of compounds resulted in some obvious binders. (**Figure 3**) with the most interesting being compounds (**14**) and (**20**). Unfortunately, compound (**20**) did not reach the required solubility threshold for the subsequent binding confirmation via ¹⁵N HSQC. On the other hand (**14**) was quite soluble up to greater than 2.5 mM in the protein buffer and was submitted for a ¹⁵N HSQC with ¹⁵N labeled HRAS (G12V). Curiously, however, compound (**15**), which was structurally very similar to the top binder compound (**14**), was not a binder. This was intriguing and merited further study. Both compounds (**14**) and (**15**) to H-Ras (G12V) (PDB: 3O1W) using MOE in an attempt to gain further insight. The results from the docking study are presented in **figure 3**.

achieved by switching from a microwave reactor to a more classical bench synthesis) increased the yield by approximately 20 % although the reaction time went from 8 minutes to 72 hours. The freebase form of (**3**), (**4**) and (**5**) were found to be unstable at room temperature over time and so they were stored and screened as the HCl salts. Subsequently, the amides and sulfonamides were rapidly synthesized in parallel using the corresponding sulfonyl and acyl chlorides respectively. An



Scheme 2: Synthesis of fragment library

The three different fluorinated bicyclic cores were screened against HRAS (G12V) (**figure 2**). The data from the DLBS experiment in figure 2 indicated that all three cores interacted weakly with HRAS (G12V) with (**4**) having the highest shift score of 3.3 Hz and (**5**) possessing the highest broadening score by visual inspection. Subsequently, with this information in hand, the screening of the *para* and *meta* analogues was prioritized.

excess of pyridine allowed for the conversion to the freebase in situ (**Scheme 2**).

Curiously, however, compound (**15**), which was structurally very similar to the top binder compound (**14**), was not a binder. This was intriguing and merited further study. Both compounds (**14**) and (**15**) to H-Ras (G12V) (PDB: 3O1W) using MOE in an attempt to gain further insight. The results from the docking study are presented in **figure 3**.

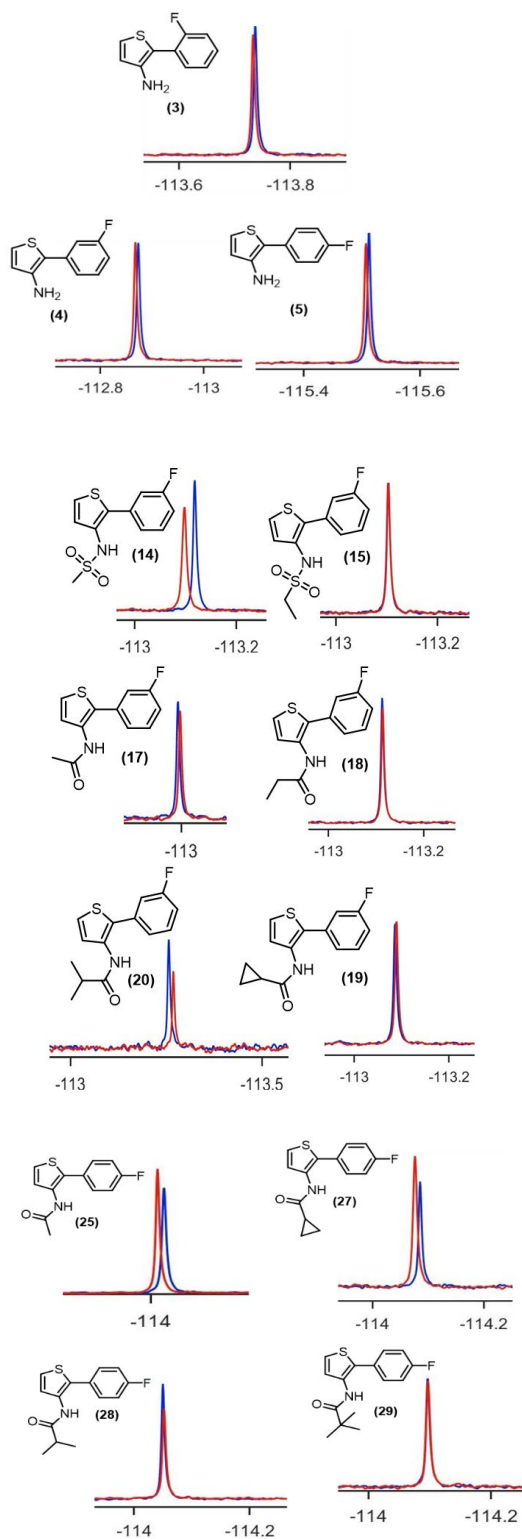


Figure 2: ^1H NMR DLBS Experiment targeting HRAS (G12V)

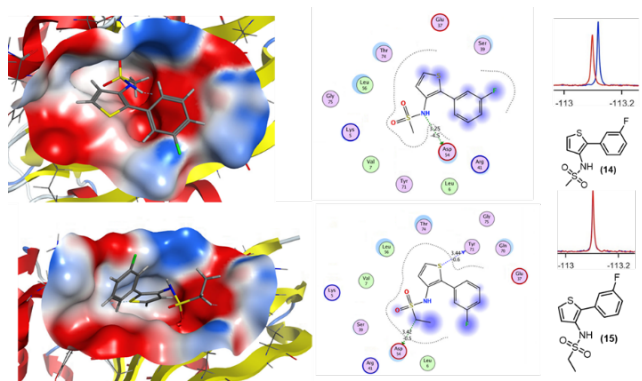


Figure 3: Molecular docking of (14) Versus (15)

The docking study indicated that the extra methylene group on the sulfonamide functionality of (15) prevents entry into the shallow pocket on HRAS (G12V) and as a result, an important hydrogen bond between the sulfonamide nitrogen and Asp 54 is prevented. This is in contrast to (14) which, because of the smaller size of the methyl substituent, is able to fit into the pocket on the protein and form the hydrogen bond between Asp 54 and the sulfonamide nitrogen. Even though (14) was more solvent exposed than (15), the hydrogen bonding interaction alone contributed approximately -4.5 kcal/mol to the overall binding energy.

Virtual screening aside, however, we wished to ensure that the interactions were at least somewhat specific to the Ras family. At this point in a fragment-based campaign, it is highly unlikely that selectivity between the mutant and wildtype HRAs or even the different isoforms KRAs or NRAs would be observed. Therefore, in order to test for binding promiscuity, the ligand (14) was screened against RNase 5 a completely unrelated protein. The result for this promiscuity ^{19}F observed ligand screen is provided in figure 4 and show that (14) does not bind to RNase 5.

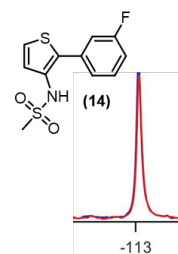


Figure 4: DLBS experiment of (14) in presence of RNase 5

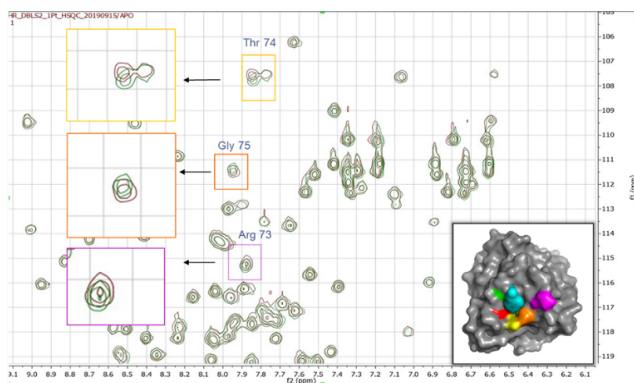


Figure 5: ^{15}N HSQC spectra overlap of HRAS (G12V) apo (green) and in presence of compound (14) (red)

Based on the HSQC results, **figure 5** confirms that compound (14) binds to HRAS (G12V). Several residues in close proximity (in space) on HRAS (G12V) had perturbations to the chemical shifts of those amino acids. These results reinforce the virtual screening results provided in **figure 3** because the residues that are seen to be affected in the HSQC experiment are the same residues that are predicted to interact with the compound to produce the best pose during the docking.

In conclusion, a previously unreported fluorinated bicyclic thiophene library has been synthesized in a modular fashion. The library was then used as the starting point of a fragment-based drug discovery campaign to target HRAS (G12V). Binders to the aforementioned protein were discovered. Solubility limits for the binders were subsequently established. Promiscuity studies were done by testing the best (and decently soluble) binder to an unrelated protein target and binding to HRAS (G12V) was confirmed with protein observed NMR spectroscopy using a ^{15}N labelled version of HRAS (G12V). Additionally, a hypothesis provided by docking explains why a very similar compound to the best binder did not bind to HRAS (G12V).

Acknowledgements

NMX Research and solutions provided a tremendous amount of support and a wealth of knowledge. The authors also appreciate the support from the FORGione group at Concordia University in Montreal for assistance with their expertise in decarboxylative cross-coupling reactions.

References

- Gillis, E. P.; Eastman, K. J.; Hill, M. D.; Donnelly, D. J.; Meanwell, N. A. Applications of Fluorine in Medicinal Chemistry. *J. Med. Chem.* **2015**, *58* (21), 8315–8359. <https://doi.org/10.1021/acs.jmedchem.5b00258>.
- Marsh, E. N. G.; Suzuki, Y. Using ^{19}F NMR to Probe Biological Interactions of Proteins and Peptides. *ACS Chem. Biol.* **2014**, *9* (6), 1242–1250. <https://doi.org/10.1021/cb500111u>.
- Wang, J.; Sánchez-Roselló, M.; Aceña, J. L.; Del Pozo, C.; Sorochinsky, A. E.; Fustero, S.; Soloshonok, V. A.; Liu, H. Fluorine in Pharmaceutical Industry: Fluorine-Containing Drugs Introduced to the Market in the Last Decade (2001-2011). *Chem. Rev.* **2014**, *114* (4), 2432–2506. <https://doi.org/10.1021/cr4002879>.
- Peng, J. W. Cross-Correlated ^{19}F Relaxation Measurements for the Study of Fluorinated Ligand-Receptor Interactions. *J. Magn. Reson.* **2001**, *153* (1), 32–47. <https://doi.org/10.1006/jmre.2001.2422>.
- Chapelin, F.; Capitini, C. M.; Ahrens, E. T. Fluorine-19 MRI for Detection and Quantification of Immune Cell Therapy for Cancer. *J. Immunother. Cancer* **2018**, *6* (1), 1–11. <https://doi.org/10.1186/s40425-018-0416-9>.
- Couch, M. J.; Ouriadov, A. V.; Albert, M. S. Pulmonary Imaging Using ^{19}F MRI of Inert Fluorinated Gases. In *Hyperpolarized and Inert Gas MRI: From Technology to Application in Research and Medicine*; Elsevier Inc., 2017; pp 279–292. <https://doi.org/10.1016/B978-0-12-803675-4.00018-X>.
- Gee, C. T.; Koleski, E. J.; Pomerantz, W. C. K. Fragment Screening and Druggability Assessment for the CBP/P300 KIX Domain through Protein-Observed ^{19}F NMR Spectroscopy. *Angew. Chemie - Int. Ed.* **2015**, *54* (12), 3735–3739. <https://doi.org/10.1002/anie.201411658>.
- Vulpetti, A.; Dalvit, C. Fluorine Local Environment: From Screening to Drug Design. *Drug Discov. Today* **2012**, *17* (15–16), 890–897. <https://doi.org/10.1016/j.drudis.2012.03.014>.
- Pellecchia, M.; Bertini, I.; Cowburn, D.; Dalvit, C.; Giralto, E.; Jahnke, W.; James, T. L.; Homans, S. W.; Kessler, H.; Luchinat, C.; Meyer, B.; Oschkinat, H.; Peng, J.; Schwalbe, H.; Siegal, G. Perspectives on NMR in Drug Discovery: A Technique Comes of Age. *Nat. Rev. Drug Discov.* **2008**, *7* (9), 738–745. <https://doi.org/10.1038/nrd2606>.
- Eaton, H. L.; Wyss, D. F. Effective Progression of Nuclear Magnetic Resonance-Detected Fragment Hits. In *Methods in Enzymology*; Academic Press Inc., 2011; Vol. 493, pp 447–468. <https://doi.org/10.1016/B978-0-12-381274-2.00017-0>.
- Laplante, S. R.; Carson, R.; Gillard, J.; Aubry, N.; Coulombe, R.; Bordeleau, S.; Bonneau, P.; Little, M.; O'Meara, J.; Beaulieu, P. L. Compound Aggregation in Drug Discovery: Implementing a Practical NMR Assay for Medicinal Chemists. *J. Med. Chem.* **2013**, *56* (12), 5142–5150. <https://doi.org/10.1021/jm400535b>.
- LaPlante, S. R.; Aubry, N.; Bolger, G.; Bonneau,

P.; Carson, R.; Coulombe, R.; Sturino, C.; Beaulieu, P. L. Monitoring Drug Self-Aggregation and Potential for Promiscuity in Off-Target In Vitro Pharmacology Screens by a Practical NMR Strategy. *J. Med. Chem.* **2013**. <https://doi.org/10.1021/jm4008714>.

- (13) Ayotte, Y.; Woo S.; LaPlante, S.R.; Practical Considerations and Guidelines for Spectral Referencing for Fluorine NMR Ligand Screening. *ACS Omega* **2022** <https://doi.org/10.1021/acsomega.2c00613>.

6 DISCUSSION

The goal of this project was twofold. The first objective was to synthesize a library of small molecules and the second objective was to screen the synthesized library against HRAS-G12V

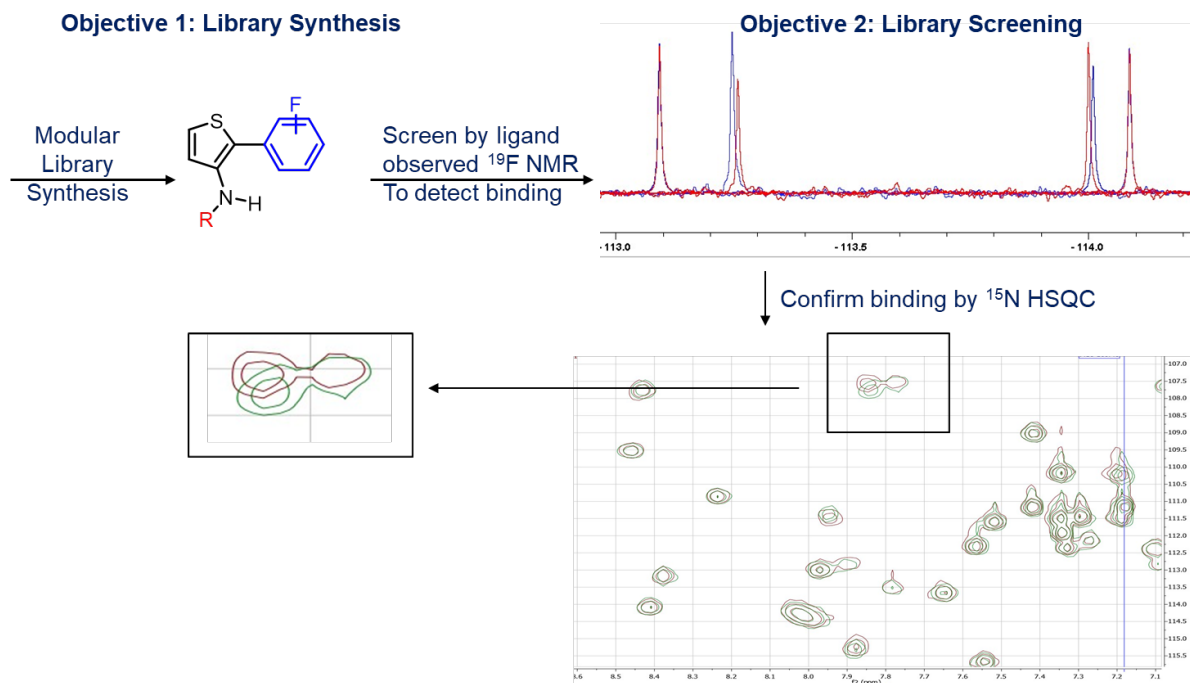


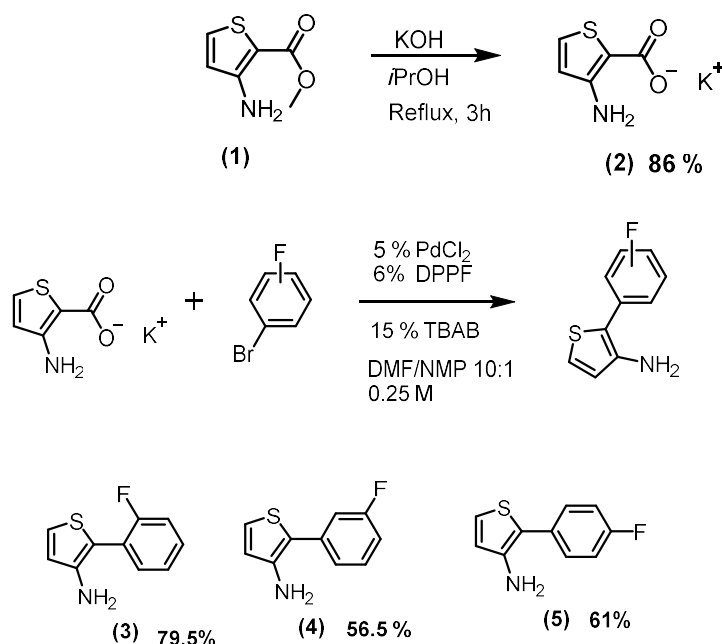
Figure 3.1 graphical abstract of project

Illustration of the overall objectives of the project. The first objective was to synthesize a library of different fluorophenyl thiophene amides and sulfonamides. The second objective was to screen the compounds by ¹⁹F NMR to detect (and subsequently confirm) binders to HRAS (G12V).

6.1 Library Synthesis

The first objective was to synthesize the various fluorophenyl thiophene amides and sulfonamides in a modular and parallel fashion. This strategy of a modular build would simplify subsequent rounds of analog synthesis if they were to be needed. The modular approach would allow for easy substitution of virtually every functionality on the fragments of interest. The parallel synthesis approach was done to reduce the amount of time necessary to synthesize and purify the library components. Adapting a literature³⁵ protocol, the bicyclic core was built using palladium catalyzed decarboxylative cross coupling using the potassium salt of 3-aminothiophene-2-carboxylate that was synthesized in house. (**Scheme 1**) Palladium decarboxylative

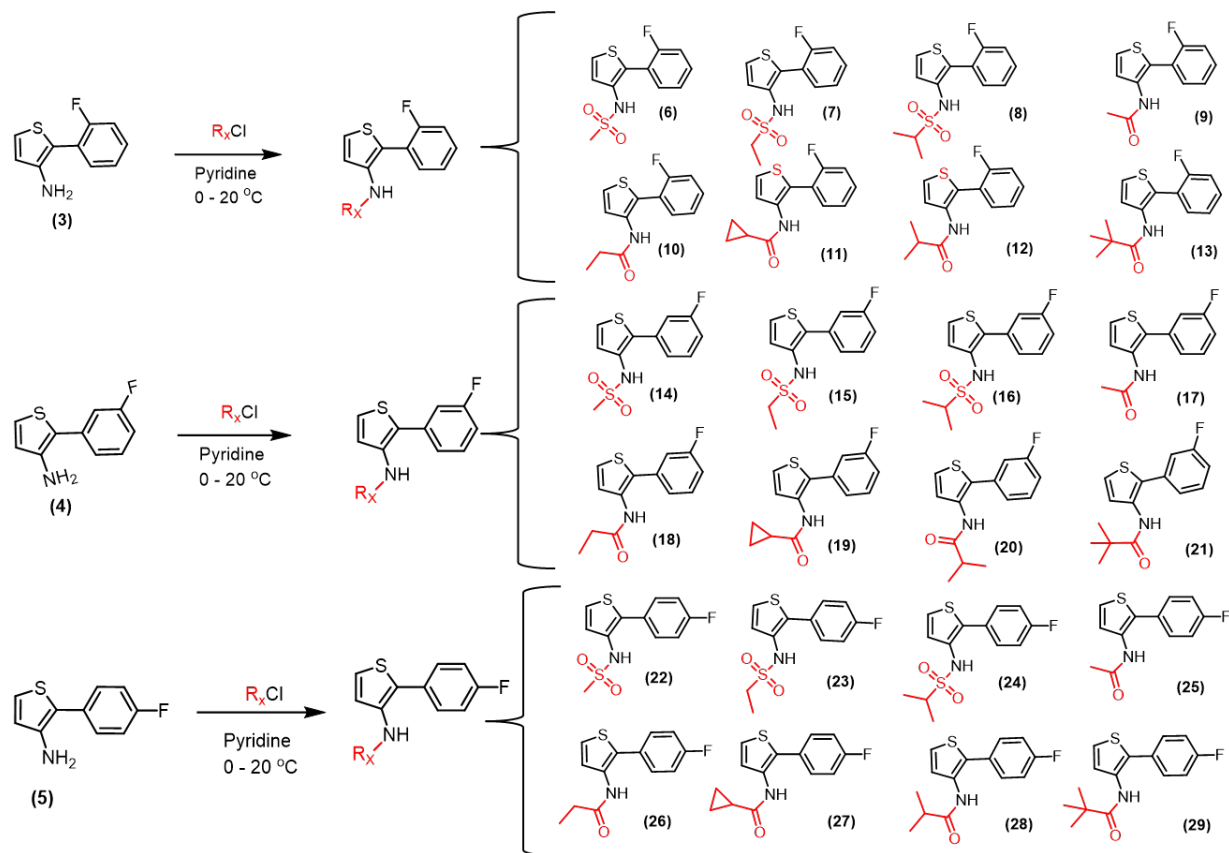
cross-coupling has several advantages over more classical palladium catalyzed cross-coupling reactions. Beginning with the starting materials themselves, compounds containing the carboxylic acid functionality tend to be relatively low cost, easily available and stable.³⁶ Secondly, decarboxylative cross-couplings extrude carbon dioxide as opposed to stoichiometric amounts of metallic waste, such as tin or magnesium in the Stille or Kumada reactions respectively.³⁷



Scheme 1: Synthesis of the three different fluorophenylthiophene cores

The yields for compound **(5)** ranged from 56-71% whereas yields for **(3)** routinely reached as high as 82%. Reaction progress monitoring by GC-MS revealed that the amount of the undesired homocoupling side product (4,4'-difluoro-1,1'-biphenyl) in the case of the para coupling reaction was higher when compared to the ortho coupling reaction explaining the reduced yield. Compounds **(3)-(5)** were not stable in their freebase form and so it was necessary to form and then store the compounds as the HCl salts. Subsequently, using the amine as a handle, the three bicyclic cores were diversified into various sulfonamides and amides. (**Scheme 2**). This chemistry was done in a crude parallel format. For each of the three series in scheme 2, 8 oven dried vials were labelled and flushed with nitrogen before the

addition of 1 mL of pyridine and 50 mg of the HCl salt of the corresponding amines **(3)**, **(4)** or **(5)**. Dissolution (and thus conversion to the free-base form) was instant. Because the reactions with acid chlorides and sulfonyl chlorides are quite exothermic, the vials were all placed on ice before addition of 1.2 equivalents of the correct sulfonyl or acid chloride to each reaction. Reaction progress was monitored by TLC and upon completion, the solvent was concentrated *in vacuo* before purification via normal phase flash column chromatography without a work-up, streamlining the process even further.



Scheme 2: diversification of bicyclic cores into a variety of sulfonamides and amides

In the past,³⁸ several thiophene containing drugs were removed due to phase IV failure as a result of reactive metabolite formation (figure 3.2). This has led to trepidation among medicinal chemists and limited usage of the thiophene ring in recent drug discovery efforts.³⁹ This trepidation has crept into fragment based drug discovery community and as a result myriad compounds that contain the five-membered thiophene ring are typically excluded from fragment based libraries flagged as “structural alerts” due to their potential to form reactive intermediates.

38,40,41

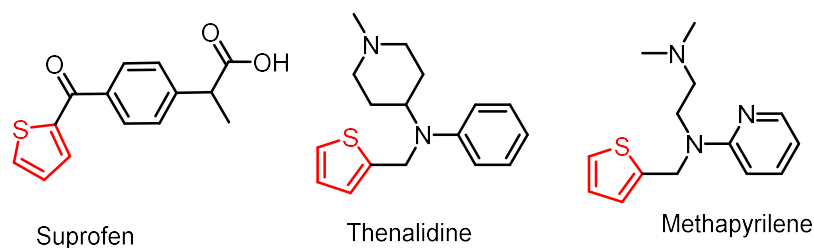


Figure 3.2: Selected examples of thiophene containing drugs that were FDA approved and subsequently had their approval revoked due to reactive metabolite formation

Recently, however, it has been shown^{42,43} that introducing an electron withdrawing group at the two position of the thiophene ring dramatically reduced the bioactivation that typically leads on to the formation of reactive metabolites. We therefore posited that it would be useful to possess such a library for our in-house fragment based medicinal chemistry projects in order to generate some potentially useful intellectual property.

6.2 Library screening

After completion of the first objective, the library synthesis, attention was diverted to the second objective, namely, binding detection via ¹⁹F ligand observed NMR screening. The choice of protein was quite important. Due to the smaller sizes, fragments tend to be dramatically more promiscuous binders⁴⁴ than drug like molecules and so had a large protein such as BSA (~65 kDa)⁴⁵ been used, it is likely that there would have been quite a high hit rate and the complexity of the 2 dimensional spectrum would have made structure based drug discovery difficult to accomplish by NMR.⁴⁶ Therefore, the choice needed to be a small “undruggable” biomolecule that has previously been validated as a viable drug discovery target. Furthermore, it would be useful to choose a protein that already had the ¹⁵N-HSQC residues assigned, which would allow for identification of the residues that interact with the ligand and facilitate subsequent rounds of structure activity relationships. All the aforementioned factors led to the use of a specific mutant in the RAS family known as H-RAS (G12V). RAS family proteins are broadly considered to be undruggable targets,⁴⁷ The ¹⁵N-HSQC of this specific H-RAS mutant was assigned at near physiological pH⁴⁸ and H-RAS (G12V) is relatively small with a size of 21 kDa.⁴⁹

The human Ras family of proteins comprises of K-Ras4A, K-Ras4B, H-Ras and N-Ras.⁴⁹ They act as molecular switches regulating several important processes such as cell growth and cell differentiation.⁵⁰ All Ras proteins are membrane bound GTPases. They regulate their respective biological processes by cycling between two states, the GTP-bound on (active) state and the

GDP-bound off (inactive) state.⁵¹ Several Ras mutations are oncogenic because they disrupt downstream signalling.⁵¹ The H-Ras (G12V) mutant is one of the most commonly encountered oncogenic mutations in human cancers, the mutation dramatically increases the GTPase activity.⁴⁹ This has led to countless, mostly fruitless, attempts at generating FDA approved Ras inhibitors for the various Ras variants and led the medicinal chemistry community to describe the Ras family as undruggable.^{47,52-55} Because of the challenges associated with targeting Ras combined with the fact that H-Ras (G12V) is a very common oncogenic mutation made H-Ras(G12V) the perfect protein for this fragment library project as the target would be a challenge to any drug discovery effort.

The initial binding detection was done via ligand observed fluorine NMR. Fluorine NMR has some advantages over proton NMR. The range of possible chemical shifts is a lot wider than that of proton NMR meaning that the throughput can be increased dramatically because more structurally similar compounds can be pooled together in one NMR sample. Furthermore, the vast majority of fluorinated organic compounds have more hydrogens than they have fluorines and coupled with a lower chemical shift range means dramatically more overlap in a proton (hydrogen) spectrum (of similar compounds) compared to the potential for overlap in a fluorine spectrum. This is illustrated in figure 3.3 which compares the proton NMR to the fluorine NMR of four structurally similar compounds. The overlap is quite apparent in the proton spectrum, whereas the four peaks on the fluorine spectrum are well resolved and separate.

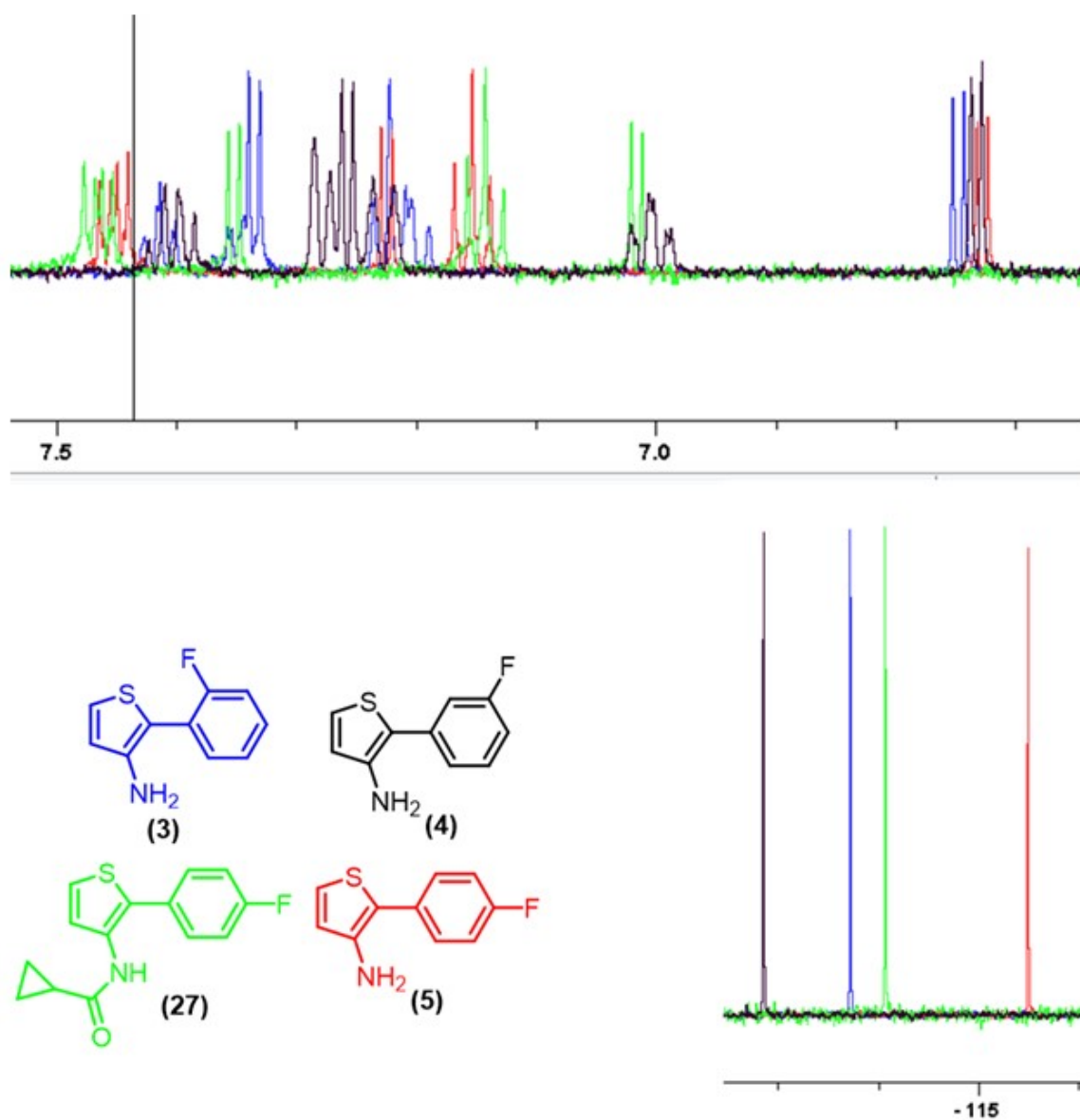


Figure 3.3 Comparison of overlapping proton and fluorine NMR spectra

Illustration showing the high overlap in proton NMR spectra (above) and the lack thereof in overlapping fluorine NMR spectra (bottom right) of four structurally similar compounds.

A selection of compounds from the synthesized library was submitted for ^{19}F NMR ligand observed binding detection studies and the results are presented in figure 3.4. Binding was detected for four compounds: **(14)**, **(20)**, **(25)** and **(27)**. Curiously, however, compound **(15)**, which was structurally very similar to the top binder compound **(14)**, was not a binder. This was intriguing and we felt that it merited further study. We therefore docked both compound **(14)** and **(15)** to H-Ras (G12V) using MOE in an attempt to gain further insight.

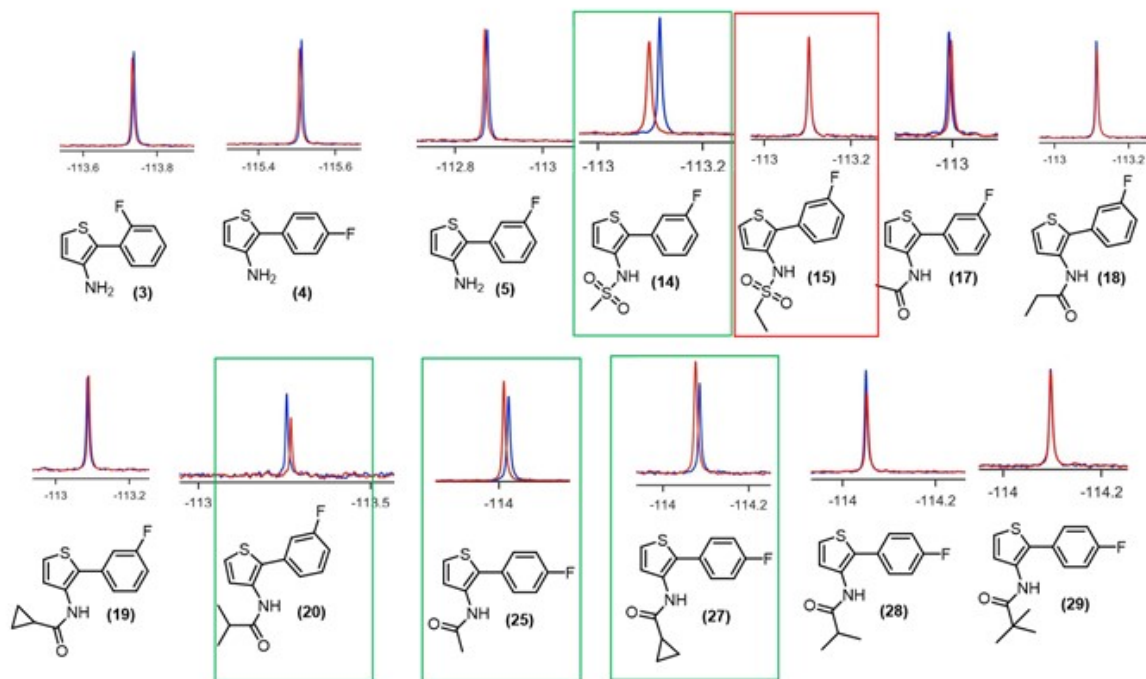


Figure 3.4 ^{19}F NMR ligand observed screening results

Compounds that were binders are identified by the green rectangles. Compound **(15)** which was structurally very similar to compound **(14)** was categorized as a non-binder and is highlighted in red.

The results from the docking study are presented in figure 3.5. The docking study indicates that the extra methylene group on the sulfonamide functionality in compound **(15)** prevents entry into the shallow pocket on HRAS (G12V) and as a result, an important hydrogen bond between the sulfonamide nitrogen and Asp 54 is prevented. This is in contrast to compound **(14)** which, because of the smaller size of the substituent, is able to fit into the shallow pocket on the protein and form the hydrogen bond between Asp 54 and the sulfonamide nitrogen. Even though **(14)** was more solvent exposed than **(15)**, the hydrogen bonding interaction alone contributed -4.5 kcal/mol to the overall binding energy.

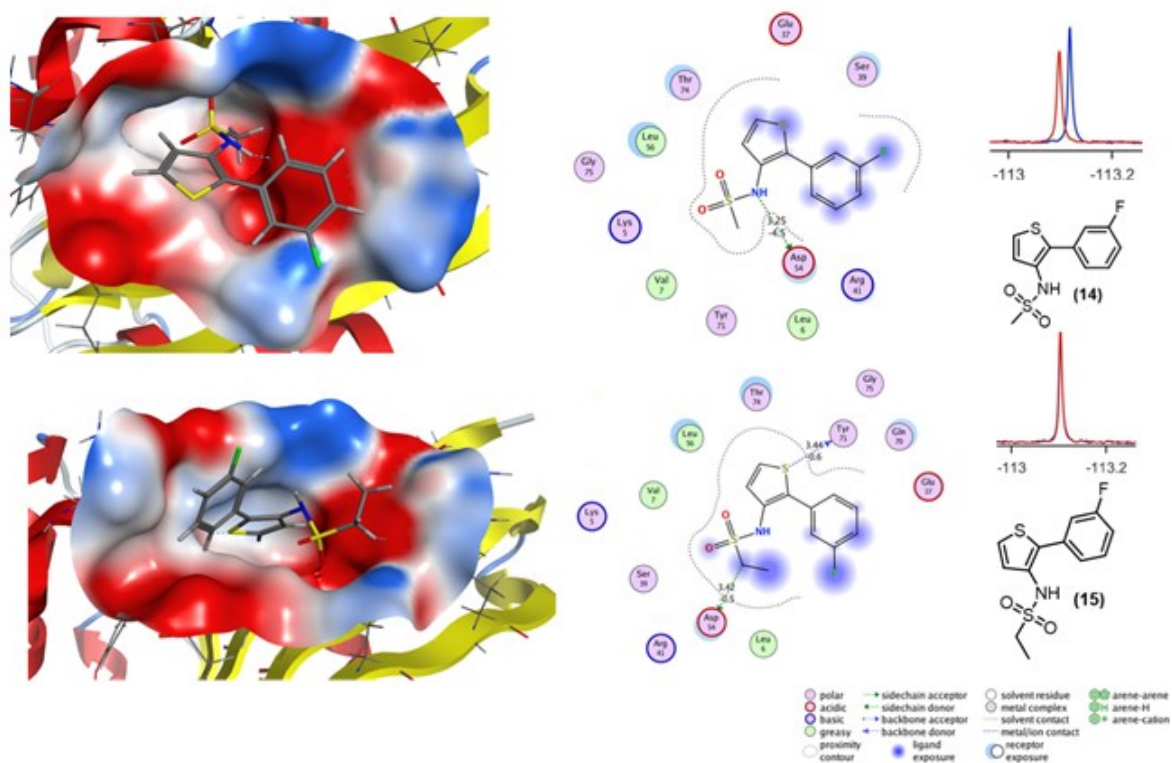
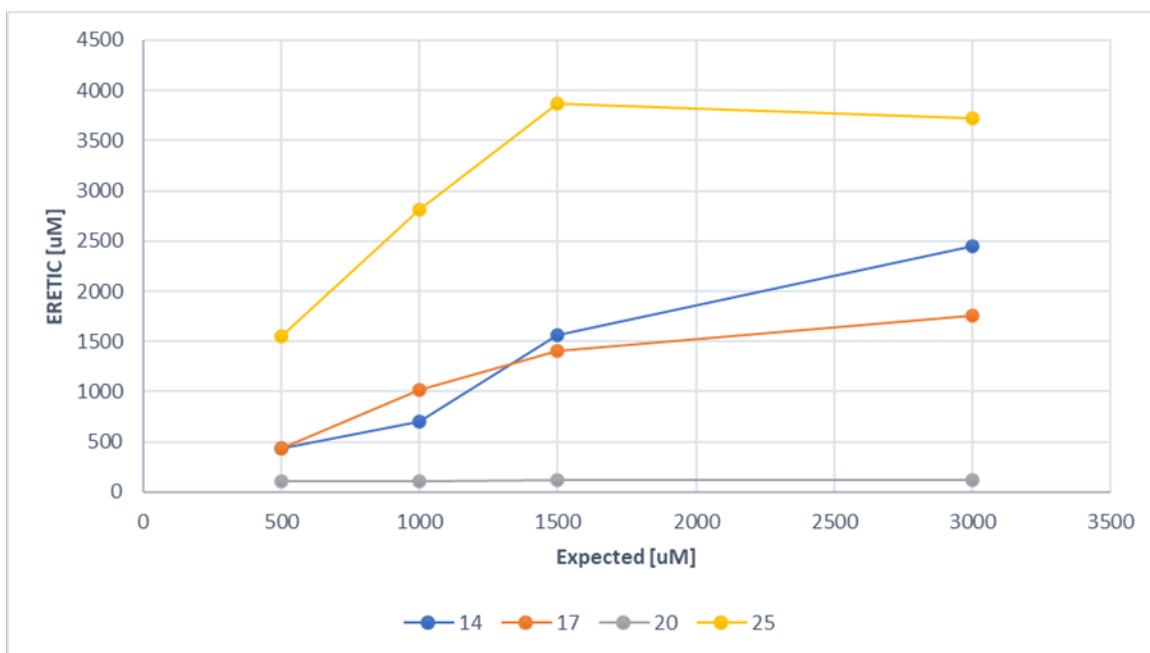


Figure 3.5 Docking results for best binder (14) and structurally similar non-binder (15)

Prior to performing the HSQC experiments, we wished to confirm the solubility of the best binders. Therefore, we determined the concentration using an external standard of maleic acid using the ERETIC method.⁵⁶ The results for this experiment are depicted in figure 3.6. They show that out of our four ¹⁹F NMR detected binders, three compounds (**14**), (**17**), and (**25**) were quite soluble up until (at least) ~2400, 1700 and 3800 μ M respectively and that one compound, (**20**), was only soluble up until ~ 100 μ M. Having a high ligand solubility is quite important for K_d determination via ¹⁵N HSQC. The compound is typically titrated, and a low solubility would not provide adequate data to obtain the dissociation constant.



	14	17	20	25
[Expected] [uM]	ERETIC [uM]	ERETIC [uM]	ERETIC [uM]	ERETIC [uM]
500	435	439.4	105.6	1555.3
1000	700	1010.9	106.2	2818.0
1500	1559	1406.7	114.7	3862.2
3000	2447	1757.9	114.6	3716.7

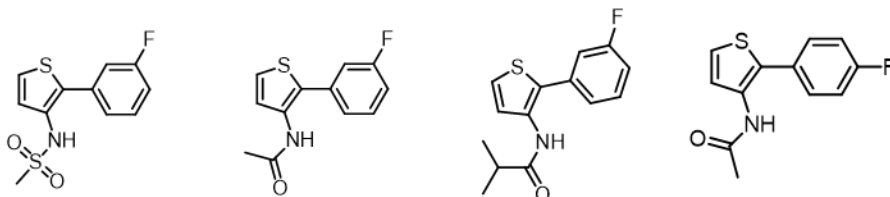


Figure 3.6 Solubility results for four ^{19}F NMR detected binders

The final test before submitting the compound to an HSQC study was the promiscuity test. We wished to ensure that the interactions were at least somewhat specific to the Ras family. At this point in a fragment-based campaign, it is highly unlikely that selectivity between the mutant and wildtype HRAS or even the different isoforms KRas or NRas would be observed. Therefore, in order to test for binding promiscuity, the ligand (**14**) was screened against RNase 5 a *completely unrelated* protein. The result for this promiscuity ^{19}F observed ligand screen is provided in figure 3.7 and show that compound (**14**) does not bind to RNase 5.

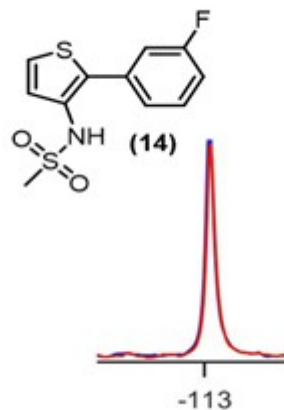


Figure 3.7 Result of promiscuity study for compound (14). Binding was not detected via ^{19}F Ligand observed NMR

Comparing the results on figure 3.7 to the binding data for compound (14) in figure 3.3, no chemical shift perturbation (broadening or shifting) can be observed for the former whereas there is a clear broadening and shift for the latter, when compound (14) was targeting HRAS (G12V).

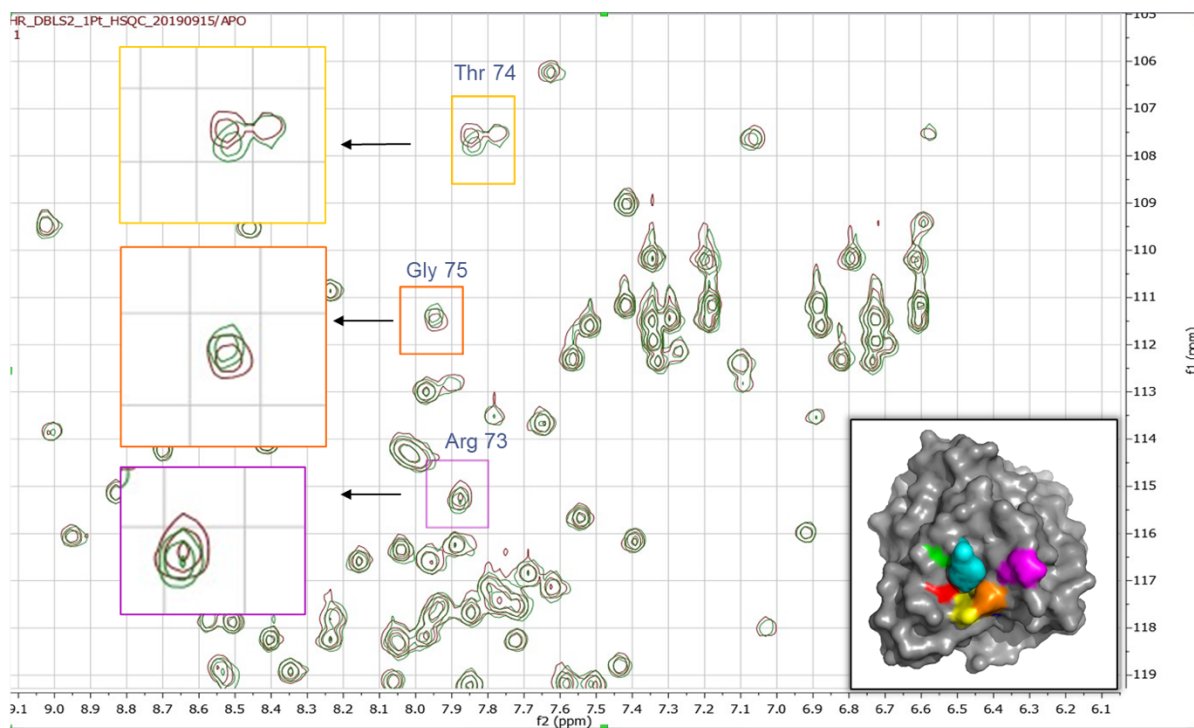


Figure 3.8 ^{15}N HSQC spectra overlap of HRAS (G12V) apo (green) and in presence of compound (14) (red)

Figure 3.8 shows the results of the ^{15}N HSQC study. Clearly visible on the figure are perturbations to the chemical shifts of several residues that are close in space a clear indication of binding.

In conclusion, a previously unreported fluorinated bicyclic thiophene library has been prepared in a modular fashion. The library was then used as the starting point of a fragment-based drug discovery campaign to target HRAS (G12V). Binders to the aforementioned protein were discovered. Solubility limits for the binders were subsequently established. Promiscuity studies were done by testing the best (and decently soluble) binder to an unrelated protein target and binding to HRAS (G12V) was confirmed with protein observed NMR spectroscopy using a ^{15}N labelled version of HRAS (G12V).

7 CONCLUSION AND PERSPECTIVES

To conclude, the purpose of this project was to synthesize a fluorinated, bicyclic, thiophene based fragment library in a modular fashion and to screen the library via ligand observed ^{19}F NMR against two proteins that are of interest to the scientific community, HRAS and RNase 5. four compounds from the library showed an affinity to HRAS (G12V) via ligand observed methods. To confirm binding to the target, the most potent fragment (**14**) was followed via an ^{15}N -HSQC experiment with ^{15}N labelled HRAS (G12V). In Figure 3.8, it is apparent that several HRAS residues have a different chemical environment in the presence of fragment (**14**) which is a clear indication of binding. Binding promiscuity was ruled out by counter screening the fragment with a protein unrelated to HRAS, RNase 5, which showed that no binding occurred.

Even though fragment (**14**) has a binding affinity for HRAS (G12V), it is far from a drug and only a starting point. Therefore, future work would require improving the potency, selectivity and pharmacokinetic profile of the candidate. There are several approaches that may lead to improved potency. One suggestion would be to screen a larger library of fragments in the presence of HRAS (G12V) and fragment (**14**) in order to find a second fragment that has affinity to HRAS with fragment (**14**) in place. If this second fragment were to be found, a crystal structure of HRAS (G12V) in the presence of both fragments would allow medicinal chemists to potentially link the fragments depending on the relative distance to one another. Another option would be to successively grow the fragment by adding substituents to various positions on the bicyclic core in order to improve affinity.

8 REFERENCES

- (1) Carpenter, S.; Rigaud, M.; Barile, M.; Priest, T. J.; Perez, L.; Ferguson, J. B. *THE EBERS PAPYRUS Possibly Having to Do With Diabetes Mellitus*; 2006.
- (2) Mehta, A. Chemical & Engineering News: Top Pharmaceuticals: Aspirin <http://pubsapp.acs.org/cen/coverstory/83/8325/8325aspirin.html?> (accessed Aug 3, 2020).
- (3) Duthie, G. G.; Wood, A. D. Natural Salicylates: Foods, Functions and Disease Prevention. <https://doi.org/10.1039/c1fo10128e>.
- (4) Sawynok, J. The Therapeutic Use of Heroin: A Review of the Pharmacological Literature. *J. Physiol. Pharmacol* **1986**, *64*, 1–6. <https://doi.org/https://doi.org/10.1139/y86-001>.
- (5) Klous, M. G.; Brink, W. Van Den; Ree, J. M. V.; Beijnen, J. H. Development of Pharmaceutical Heroin Preparations for Medical Co-Prescription to Opioid Dependent Patients. *Drug and Alcohol Dependence*. Elsevier December 12, 2005, pp 283–295. <https://doi.org/10.1016/j.drugalcdep.2005.04.008>.
- (6) Inturrisi, C. E.; Schultz, M.; Shin, S.; Umans, J. G.; Angel, L.; Simon, E. J. Evidence from Opiate Binding Studies That Heroin Acts through Its Metabolites. *Life Sci.* **1983**, *33* (SUPPL. 1), 773–776. [https://doi.org/10.1016/0024-3205\(83\)90616-1](https://doi.org/10.1016/0024-3205(83)90616-1).
- (7) Bohacek, R. S.; McMartin, C.; Guida, W. C. The Art and Practice of Structure-based Drug Design: A Molecular Modeling Perspective. *Med. Res. Rev.* **1996**, *16* (1), 3–50. [https://doi.org/10.1002/\(SICI\)1098-1128\(199601\)16:1<3::AID-MED1>3.0.CO;2-6](https://doi.org/10.1002/(SICI)1098-1128(199601)16:1<3::AID-MED1>3.0.CO;2-6).
- (8) Hann, M. M.; Oprea, T. I. Pursuing the Leadlikeness Concept in Pharmaceutical Research. *Current Opinion in Chemical Biology*. Elsevier Current Trends June 1, 2004, pp 255–263. <https://doi.org/10.1016/j.cbpa.2004.04.003>.
- (9) Eaton, H. L.; Wyss, D. F. Effective Progression of Nuclear Magnetic Resonance-Detected Fragment Hits. In *Methods in Enzymology*; Academic Press Inc., 2011; Vol. 493, pp 447–468. <https://doi.org/10.1016/B978-0-12-381274-2.00017-0>.
- (10) Fink, T.; Bruggesser, H.; Reymond, J. L. Virtual Exploration of the Small-Molecule Chemical Universe below 160 Daltons. *Angew. Chemie - Int. Ed.* **2005**, *44* (10), 1504–1508. <https://doi.org/10.1002/anie.200462457>.

- (11) Fink, T.; Raymond, J. L. Virtual Exploration of the Chemical Universe up to 11 Atoms of C, N, O, F: Assembly of 26.4 Million Structures (110.9 Million Stereoisomers) and Analysis for New Ring Systems, Stereochemistry, Physicochemical Properties, Compound Classes, and Drug Discovery. *J. Chem. Inf. Model.* **2007**, *47* (2), 342–353. <https://doi.org/10.1021/ci600423u>.
- (12) Murray, C. W.; Rees, D. C. The Rise of Fragment-Based Drug Discovery. *Nat. Chem.* **2009**, *1* (3), 187–192. <https://doi.org/10.1038/nchem.217>.
- (13) Murray, C. W.; Verdonk, M. L.; Rees, D. C. Experiences in Fragment-Based Drug Discovery. *Trends in Pharmacological Sciences*. Elsevier Current Trends May 1, 2012, pp 224–232. <https://doi.org/10.1016/j.tips.2012.02.006>.
- (14) Lipinski, C. A.; Lombardo, F.; Dominy, B. W.; Feeney, P. J. Experimental and Computational Approaches to Estimate Solubility and Permeability in Drug Discovery and Development Settings. *Adv. Drug Deliv. Rev.* **1997**, *23*, 3–25. [https://doi.org/10.1016/S0169-409X\(00\)00129-0](https://doi.org/10.1016/S0169-409X(00)00129-0).
- (15) Veber, D. F.; Johnson, S. R.; Cheng, H.; Smith, B. R.; Ward, K. W.; Kopple, K. D. Molecular Properties That Influence the Oral Bioavailability of Drug Candidates. *J. Med. Chem.* **2002**, *45*, 2615–2623. <https://doi.org/10.1021/jm020017n>.
- (16) Congreve, M.; Carr, R.; Murray, C.; Jhoti, H. A “Rule of Three” for Fragment-Based Lead Discovery? *Drug Discovery Today*. October 1, 2003, pp 876–877. [https://doi.org/10.1016/S1359-6446\(03\)02831-9](https://doi.org/10.1016/S1359-6446(03)02831-9).
- (17) Lipitor - The World’s All-Time Best Selling Drug | TSC <https://theskepticalchemist.com/lipitor-worlds-all-time-best-selling-drug/> (accessed Aug 16, 2020).
- (18) Duong-Thi, M. D.; Bergström, M.; Fex, T.; Isaksson, R.; Ohlson, S. High-Throughput Fragment Screening by Affinity LC-MS. *J. Biomol. Screen.* **2013**, *18* (2), 160–171. <https://doi.org/10.1177/1087057112459271>.
- (19) Hajduk, P. J.; Sheppard, G.; Nettlesheim, D. G.; Olejniczak, E. T.; Shuker, S. B.; Meadows, R. P.; Steinman, D. H.; Carrera, G. M.; Marcotte, P. A.; Severin, J.; Walter, K.; Smith, H.; Gubbins, E.; Simmer, R.; Holzman, T. F.; Morgan, D. W.; Davidsen, S. K.; Summers, J. B.; Fesik, S. W. Discovery of Potent Nonpeptide Inhibitors of Stromelysin Using SAR by NMR. *J. Am. Chem. Soc.* **1997**, *119* (25), 5818–5827.

- <https://doi.org/10.1021/ja9702778>.
- (20) Giannetti, A. M. From Eperimental Design to Validated Hits: A Comprehensive Walk-through of Fragment Lead Identification Using Surface Plasmon Resonance. In *Methods in Enzymology*; Academic Press Inc., 2011; Vol. 493, pp 169–218. <https://doi.org/10.1016/B978-0-12-381274-2.00008-X>.
- (21) Neumann, L.; Von Knig, K.; Ullmann, D. HTS Reporter Displacement Assay for Fragment Screening and Fragment Evolution toward Leads with Optimized Binding Kinetics, Binding Selectivity, and Thermodynamic Signature. In *Methods in Enzymology*; Academic Press Inc., 2011; Vol. 493, pp 299–320. <https://doi.org/10.1016/B978-0-12-381274-2.00012-1>.
- (22) Seidel, S. A. I.; Dijkman, P. M.; Lea, W. A.; van den Bogaart, G.; Jerabek-Willemsen, M.; Lazic, A.; Joseph, J. S.; Srinivasan, P.; Baaske, P.; Simeonov, A.; Katritch, I.; Melo, F. A.; Ladbury, J. E.; Schreiber, G.; Watts, A.; Braun, D.; Duhr, S. Microscale Thermophoresis Quantifies Biomolecular Interactions under Previously Challenging Conditions. *Methods*. Academic Press Inc. March 1, 2013, pp 301–315. <https://doi.org/10.1016/j.ymeth.2012.12.005>.
- (23) Spurlino, J. C. Fragment Screening Purely with Protein Crystallography. In *Methods in Enzymology*; Academic Press Inc., 2011; Vol. 493, pp 321–356. <https://doi.org/10.1016/B978-0-12-381274-2.00013-3>.
- (24) Lepre, C. A. Practical Aspects of NMR-Based Fragment Screening. In *Methods in Enzymology*; Academic Press Inc., 2011; Vol. 493, pp 219–239. <https://doi.org/10.1016/B978-0-12-381274-2.00009-1>.
- (25) The Nobel Prize in Physics 1944 - NobelPrize.org <https://www.nobelprize.org/prizes/physics/1944/summary/> (accessed Aug 20, 2020).
- (26) Rabi, I. I.; Zacharias, J. R.; Millman, S.; Kusch, P. A New Method of Measuring Nuclear Magnetic Moment [5]. *Physical Review*. American Physical Society February 15, 1938, p 318. <https://doi.org/10.1103/PhysRev.53.318>.
- (27) The Nobel Prize in Physics 1952 <https://www.nobelprize.org/prizes/physics/1952/summary/> (accessed Aug 20, 2020).
- (28) Keeler, J. *Understanding NMR Spectroscopy*.
- (29) Pellecchia, M.; Sem, D. S.; Wüthrich, K. NMR in Drug Discovery. *Nature Reviews Drug*

- Discovery*. European Association for Cardio-Thoracic Surgery 2002, pp 211–219. <https://doi.org/10.1038/nrd748>.
- (30) Kleckner, I. R.; Foster, M. P. An Introduction to NMR-Based Approaches for Measuring Protein Dynamics. *Biochimica et Biophysica Acta - Proteins and Proteomics*. Biochim Biophys Acta August 2011, pp 942–968. <https://doi.org/10.1016/j.bbapap.2010.10.012>.
- (31) Meyer, B.; Peters, T. NMR Spectroscopy of Proteins NMR Spectroscopy Techniques for Screening and Identifying Ligand Binding to Protein Re1. B. Meyer and T. Peters, 2003, 864–890. *Ceptors Angewandte*. **2003**, No. 8, 864–890.
- (32) Williamson, M. P. Using Chemical Shift Perturbation to Characterise Ligand Binding. *Progress in Nuclear Magnetic Resonance Spectroscopy*. Elsevier B.V. August 2013, pp 1–16. <https://doi.org/10.1016/j.pnmrs.2013.02.001>.
- (33) Williamson, M. P. Using Chemical Shift Perturbation to Characterise Ligand Binding. *Prog. Nucl. Magn. Reson. Spectrosc.* **2013**, 73, 1–16. <https://doi.org/10.1016/j.pnmrs.2013.02.001>.
- (34) Williamson, M. P. Using Chemical Shift Perturbation to Characterise Ligand Binding. *Progress in Nuclear Magnetic Resonance Spectroscopy*. Elsevier B.V. 2013, pp 1–16. <https://doi.org/10.1016/j.pnmrs.2013.02.001>.
- (35) Mitchell, D.; Coppert, D. M.; Moynihan, H. A.; Lorenz, K. T.; Kissane, M.; McNamara, O. A.; Maguire, A. R. A Practical Synthesis of Biaryls via a Thermal Decarboxylative Pd-Catalyzed Cross-Coupling Reaction Operating at Moderate Temperature. *Org. Process Res. Dev.* **2011**, 15 (5), 981–985. <https://doi.org/10.1021/op200030t>.
- (36) Rodríguez, N.; Goossen, L. J. Decarboxylative Coupling Reactions: A Modern Strategy for C–C-Bond Formation. *Chem. Soc. Rev.* **2011**, 40 (10), 5030–5048. <https://doi.org/10.1039/c1cs15093f>.
- (37) Johansson Seechurn, C. C. C.; Kitching, M. O.; Colacot, T. J.; Snieckus, V. Palladium-Catalyzed Cross-Coupling: A Historical Contextual Perspective to the 2010 Nobel Prize. *Angewandte Chemie - International Edition*. John Wiley & Sons, Ltd May 21, 2012, pp 5062–5085. <https://doi.org/10.1002/anie.201107017>.
- (38) Jaladanki, C. K.; Taxak, N.; Varikoti, R. A.; Bharatam, P. V. Toxicity Originating from Thiophene Containing Drugs: Exploring the Mechanism Using Quantum Chemical Methods. *Chem. Res. Toxicol.* **2015**, 28 (12), 2364–2376.

<https://doi.org/10.1021/acs.chemrestox.5b00364>.

- (39) Kalgutkar, A. S. Designing around Structural Alerts in Drug Discovery. *Journal of Medicinal Chemistry*. American Chemical Society June 25, 2020, pp 6276–6302. <https://doi.org/10.1021/acs.jmedchem.9b00917>.
- (40) Dang, N. Le; Hughes, T. B.; Miller, G. P.; Swamidass, S. J. Computational Approach to Structural Alerts: Furans, Phenols, Nitroaromatics, and Thiophenes. *Chem. Res. Toxicol.* **2017**, *30* (4), 1046–1059. <https://doi.org/10.1021/acs.chemrestox.6b00336>.
- (41) Limban, C.; Nuță, D. C.; Chiriță, C.; Negreș, S.; Arsene, A. L.; Goumenou, M.; Karakitsios, S. P.; Tsatsakis, A. M.; Sarigiannis, D. A. The Use of Structural Alerts to Avoid the Toxicity of Pharmaceuticals. *Toxicology Reports*. Elsevier Inc. January 1, 2018, pp 943–953. <https://doi.org/10.1016/j.toxrep.2018.08.017>.
- (42) Chen, W.; Caceres-Cortes, J.; Zhang, H.; Zhang, D.; Humphreys, W. G.; Gan, J. Bioactivation of Substituted Thiophenes Including α -Chlorothiophene- Containing Compounds in Human Liver Microsomes. *Chem. Res. Toxicol.* **2011**, *24* (5), 663–669. <https://doi.org/10.1021/tx100386z>.
- (43) Shu, Y. Z.; Johnson, B. M.; Yang, T. J. Role of Biotransformation Studies in Minimizing Metabolism-Related Liabilities in Drug Discovery. *AAPS Journal*. Springer March 13, 2008, pp 178–192. <https://doi.org/10.1208/s12248-008-9016-9>.
- (44) Klessig, D. F.; Tian, M.; Choi, H. W. Multiple Targets of Salicylic Acid and Its Derivatives in Plants and Animals. *Frontiers in Immunology*. Frontiers Media S.A. 2016, p 206. <https://doi.org/10.3389/fimmu.2016.00206>.
- (45) Majorek, K. A.; Porebski, P. J.; Dayal, A.; Zimmerman, M. D.; Jablonska, K.; Stewart, A. J.; Chruszcz, M.; Minor, W. Structural and Immunologic Characterization of Bovine, Horse, and Rabbit Serum Albumins. *Mol. Immunol.* **2012**, *52* (3–4), 174–182. <https://doi.org/10.1016/j.molimm.2012.05.011>.
- (46) Mayer, M.; Meyer, B. Characterization of Ligand Binding by Saturation Transfer Difference NMR Spectroscopy. *Angew. Chemie - Int. Ed.* **1999**, *38* (12), 1784–1788. [https://doi.org/10.1002/\(SICI\)1521-3773\(19990614\)38:12<1784::AID-ANIE1784>3.0.CO;2-Q](https://doi.org/10.1002/(SICI)1521-3773(19990614)38:12<1784::AID-ANIE1784>3.0.CO;2-Q).
- (47) Kessler, D.; Gmachl, M.; Mantoulidis, A.; Martin, L. J.; Zoephel, A.; Mayer, M.; Gollner, A.; Covini, D.; Fischer, S.; Gerstberger, T.; Gmaschitz, T.; Goodwin, C.; Greb, P.; Häring,

- D.; Hela, W.; Hoffmann, J.; Karolyi-Oezguer, J.; Knesl, P.; Kornigg, S.; Koegl, M.; Kousek, R.; Lamarre, L.; Moser, F.; Munico-Martinez, S.; Peinsipp, C.; Phan, J.; Rinnenthal, J.; Sai, J.; Salamon, C.; Scherbantin, Y.; Schipany, K.; Schnitzer, R.; Schrenk, A.; Sharps, B.; Siszler, G.; Sun, Q.; Waterson, A.; Wolkerstorfer, B.; Zeeb, M.; Pearson, M.; Fesik, S. W.; McConnell, D. B. Drugging an Undruggable Pocket on KRAS. *Proc. Natl. Acad. Sci. U. S. A.* **2019**, *116* (32), 15823–15829. <https://doi.org/10.1073/pnas.1904529116>.
- (48) Smith, M. J.; Neel, B. G.; Ikura, M. NMR-Based Functional Profiling of RASopathies and Oncogenic RAS Mutations. *Proc. Natl. Acad. Sci. U. S. A.* **2013**, *110* (12), 4574–4579. <https://doi.org/10.1073/pnas.1218173110>.
- (49) Amin, N.; Chiarparin, E.; Coyle, J.; Nietlispach, D.; Williams, G. 1H, 15N and 13C Backbone Assignments of GDP-Bound Human H-Ras Mutant G12V. *Biomol. NMR Assign.* **2016**, *10* (1), 121–123. <https://doi.org/10.1007/s12104-015-9649-4>.
- (50) Vetter, I. R.; Wittinghofer, A. The Guanine Nucleotide-Binding Switch in Three Dimensions. *Science*. American Association for the Advancement of Science November 9, 2001, pp 1299–1304. <https://doi.org/10.1126/science.1062023>.
- (51) Karnoub, A. E.; Weinberg, R. A. Ras Oncogenes: Split Personalities. *Nature Reviews Molecular Cell Biology*. Nature Publishing Group July 2008, pp 517–531. <https://doi.org/10.1038/nrm2438>.
- (52) Stephen, A. G.; Esposito, D.; Bagni, R. G.; McCormick, F. Dragging Ras Back in the Ring. *Cancer Cell* **2014**, *25* (3), 272–281. <https://doi.org/10.1016/j.ccr.2014.02.017>.
- (53) Cox, A. D.; Der, C. J. Ras History: The Saga Continues. *Small GTPases* **2010**, *1* (1), 2–27. <https://doi.org/10.4161/sgtp.1.1.12178>.
- (54) Lu, S.; Jang, H.; Zhang, J.; Nussinov, R. Inhibitors of Ras-SOS Interactions. *ChemMedChem* **2016**, *11* (8), 814–821. <https://doi.org/10.1002/cmdc.201500481>.
- (55) Hobbs, G. A.; Der, C. J.; Rossman, K. L. RAS Isoforms and Mutations in Cancer at a Glance. *Journal of Cell Science*. **2016**, pp 1287–1292. <https://doi.org/10.1242/jcs.182873>.
- (56) Akoka, S.; Barantin, L.; Trierweiler, M. Concentration Measurement by Proton NMR Using the ERETIC Method. *Anal. Chem.* **1999**, *71* (13), 2554–2557. <https://doi.org/10.1021/ac981422i>.
- (57) Moore, A.R., Rosenberg, S.C., McCormick, F. *et al.* RAS-targeted therapies: is the

undruggable drugged?. *Nat Rev Drug Discov*, **2020**, **19**, 533–552 (2020).
<https://doi.org/10.1038/s41573-020-0068-6>

- (58) Li, W. et al. A new function for a phosphotyrosine phosphatase: linking GRB2-Sos to a receptor tyrosine kinase. *Mol. Cell. Biol.* **1994** 14, 509–517 .
-

SUPPLEMENTAL INFORMATION

Synthesis of a fluorinated library applied to fragment-based drug discovery via ¹⁹F NMR with confirmed binding to HRAS-G12V

David Bendahan, Pat Forgione, Steven R. LaPlante.

GENERAL CONDITIONS AND INSTRUMENTATION	53
SYNTHESIS	53
SYNTHESIS OF POTASSIUM 3-AMINOTHIOPHENE-2-CARBOXYLATE (2)	53
SYNTHESIS OF 2-(2-FLUOROPHENYL)THIOPHEN-3-AMINE (3):	54
SYNTHESIS OF 2-(3-FLUOROPHENYL)THIOPHEN-3-AMINE (4):	55
SYNTHESIS OF 2-(4-FLUOROPHENYL)THIOPHEN-3-AMINE (5):	55
SYNTHESIS OF N-(2-(2-FLUOROPHENYL)THIOPHEN-3-YL)METHANESULFONAMIDE (6)	56
SYNTHESIS OF N-(2-(2-FLUOROPHENYL)THIOPHEN-3-YL)ETHANESULFONAMIDE (7)	57
SYNTHESIS OF N-(2-(2-FLUOROPHENYL)THIOPHEN-3-YL)PROPANE-2-SULFONAMIDE (8)	57
SYNTHESIS OF N-(2-(2-FLUOROPHENYL)THIOPHEN-3-YL)ACETAMIDE (9)	58
SYNTHESIS OF N-(2-(2-FLUOROPHENYL)THIOPHEN-3-YL)PROPIONAMIDE (10)	58
SYNTHESIS OF N-(2-(2-FLUOROPHENYL)THIOPHEN-3-YL)ISOBUTYRAMIDE (12)	60
SYNTHESIS OF N-(2-(2-FLUOROPHENYL)THIOPHEN-3-YL)PIVALAMIDE (13)	60
SYNTHESIS OF N-(2-(3-FLUOROPHENYL)THIOPHEN-3-YL)METHANESULFONAMIDE (14)	61
SYNTHESIS OF N-(2-(3-FLUOROPHENYL)THIOPHEN-3-YL)ETHANESULFONAMIDE (15)	61
SYNTHESIS OF N-(2-(3-FLUOROPHENYL)THIOPHEN-3-YL)PROPANE-2-SULFONAMIDE (16)	62
SYNTHESIS OF N-(2-(3-FLUOROPHENYL)THIOPHEN-3-YL)ACETAMIDE (17)	63
SYNTHESIS OF N-(2-(3-FLUOROPHENYL)THIOPHEN-3-YL)PROPIONAMIDE (18)	63
SYNTHESIS OF N-(2-(3-FLUOROPHENYL)THIOPHEN-3-YL)ISOBUTYRAMIDE (20)	64
SYNTHESIS OF N-(2-(3-FLUOROPHENYL)THIOPHEN-3-YL)PIVALAMIDE (21)	65
SYNTHESIS OF N-(2-(4-FLUOROPHENYL)THIOPHEN-3-YL)METHANESULFONAMIDE (22)	66
SYNTHESIS OF N-(2-(4-FLUOROPHENYL)THIOPHEN-3-YL)ETHANESULFONAMIDE (23)	66
SYNTHESIS OF N-(2-(4-FLUOROPHENYL)THIOPHEN-3-YL)PROPANE-2-SULFONAMIDE (24)	67
SYNTHESIS OF N-(2-(4-FLUOROPHENYL)THIOPHEN-3-YL)ACETAMIDE (25)	67
SYNTHESIS OF N-(2-(4-FLUOROPHENYL)THIOPHEN-3-YL)PROPIONAMIDE (26)	68

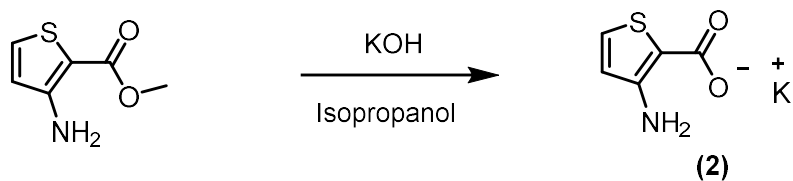
SYNTHESIS OF N-(2-(4-FLUOROPHENYL)THIOPHEN-3-YL)CYCLOPROPANECARBOXAMIDE (27).....	68
SYNTHESIS OF N-(2-(4-FLUOROPHENYL)THIOPHEN-3-YL)ISOBUTYRAMIDE (28)	69
SYNTHESIS OF N-(2-(4-FLUOROPHENYL)THIOPHEN-3-YL)PIVALAMIDE (29)	69

GENERAL CONDITIONS AND INSTRUMENTATION

All glassware was flame dried prior to reaction set up unless otherwise stated. Solids were weighed open to air and added to septa sealed round bottom flasks which was then purged with nitrogen gas. Liquids were transferred using stainless steel needles and glass or plastic syringes to maintain the inert atmosphere. Flash chromatography was carried out using the Biotage isolera system using prepackaged silica columns containing 40-63 μ m silica gel. All solvents were ACS grade and were purchased from Sigma Aldrich and used as is. All reactions were carried out under an inert atmosphere of argon or nitrogen. ^1H NMR (600 MHz) spectra and ^1H NMR (500 MHz) spectra were recorded on Bruker Avance III 600 equipped with a helium cryoprobe and a Varian Inova 500 MHz spectrometer respectively. ^{19}F NMR (564 MHz) spectra were recorded on a Bruker Avance III 600 spectrometer in proton-decoupled mode. All spectra were recorded at 25 Celsius.

SYNTHESIS

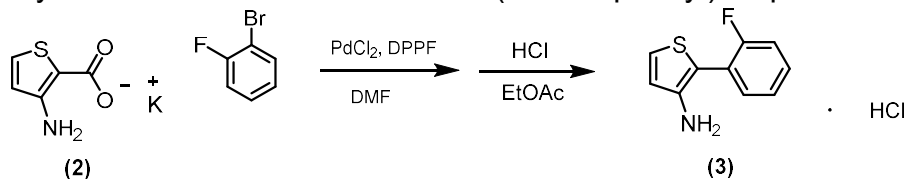
8.1 Synthesis of potassium 3-Aminothiophene-2-carboxylate (2)



15 mL of Isopropyl alcohol was added to a to a 50 mL round bottom flask containing methyl 3-aminothiophene-2- carboxylate (2.00 grams, 12.7 mmol). KOH (0.892 g, 15.9 mmol) was added, followed by more isopropyl alcohol (5 mL), and the mixture was heated to reflux for 2 hours under a nitrogen atmosphere. Subsequently, the reaction mixture was cooled in an ice bath for 30 min. The reaction mixture was vacuum filtered, and the residue was rinsed with very cold

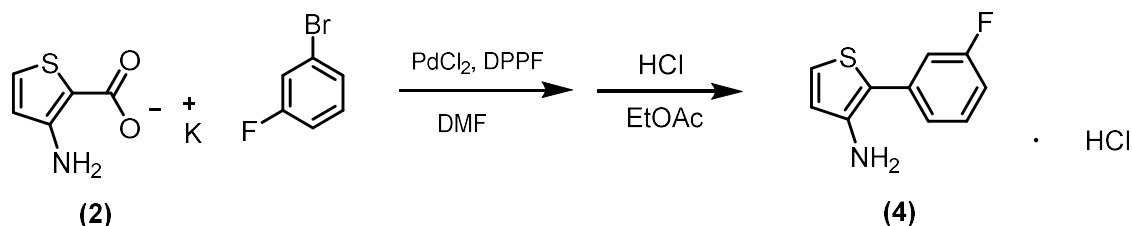
isopropanol (2x 5 mL). **(2)** was produced as a light beige solid (1.97 g, 86 %) ¹H NMR (600 MHz, DMSO) δ 6.96 – 6.92 (m, 1H), 6.43 (d, *J* = 5.5 Hz, 2H), 5.85 – 5.75 (m, 1H).

8.2 Synthesis of 2-(2-fluorophenyl)thiophen-3-amine **(3)**:



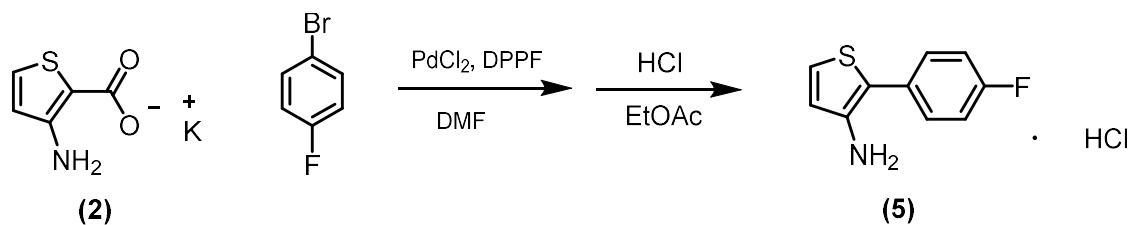
A 3-necked 25 mL round bottomed flask was evacuated and backfilled with nitrogen. DMF (9 mL) and NMP (1 mL) were added under a flow of nitrogen. Potassium 3-aminothiophene-2-carboxylate (**2**) (500 mg, 2.76 mmol), 1-bromo-2-fluorobenzene (328 μ L, 3 mmol), tetra-*n*-butylammonium bromide (133 mg, 0.414 mmol), 1,1'-bis(diphenylphosphino)ferrocene (91.9 mg, 0.166 mmol), and palladium(II) chloride (24.5 mg, 0.14 mmol) were added under a flow of nitrogen. The vessel was then evacuated and backfilled three times. The resulting mixture was heated at 80 Celsius for 72 hours. The reaction mixture was allowed to cool to room temperature. Celite (15 g) and water (150 mL) were added to the reaction mixture and stirred for 10 min. The mixture was filtered through a bed of Celite (8 g). The reaction vessel and Celite cake were rinsed with Ethyl acetate (150 mL). The layers were separated, and the aqueous layer was washed with Ethyl acetate (3 x 50 mL). The combined EtOAc layers were washed with water (4 x 150 mL) and brine (3 x 150 mL). After drying with sodium sulfate, the Ethyl acetate layer was concentrated on a rotary evaporator to and flash column chromatography was performed in a gradient of dichloromethane in hexanes (0 - 30%). All fractions containing the product were pooled and a solution of HCl in ethyl acetate was added dropwise over 20 min at 0 Celsius. A white solid precipitated out of solution almost immediately. The white solid was vacuum filtered and dried under vacuum to produce 2-(2-fluorophenyl)thiophen-3-amine hydrochloride (505 mg, 79.5 % yield). ¹H NMR (600 MHz, DMSO) δ 7.76 (t, *J* = 4.5 Hz, 1H), 7.68 – 7.61 (m, 1H), 7.54 – 7.48 (m, 1H), 7.38 (ddd, *J* = 10.7, 8.4, 1.2 Hz, 1H), 7.33 (td, *J* = 7.5, 1.2 Hz, 1H), 7.14 (s, 1H).

8.3 Synthesis of 2-(3-fluorophenyl)thiophen-3-amine (4):



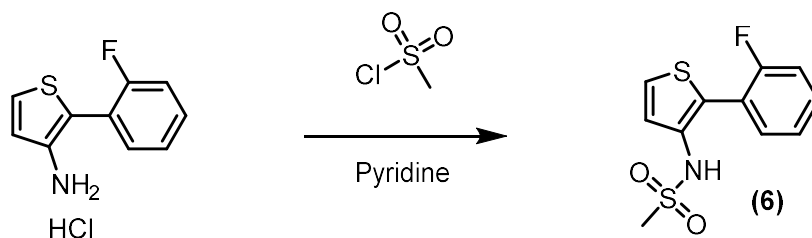
A 3-necked 25 mL round bottomed flask was evacuated and backfilled with nitrogen. DMF (16 mL) and NMP (1.6 mL) were added under a flow of nitrogen. Potassium 3-aminothiophene-carboxylate (**2**) (750 mg, 4.14 mmol), 1-bromo-3-fluorobenzene (505 μ L, 4.5 mmol), tetra-*n*-butylammonium bromide (37.5 mg, 0.1125 mmol), 1,1'-bis(diphenylphosphino)ferrocene (124.5 mg, 0.225 mmol), and palladium(II) chloride (37 mg, 0.206 mmol) were added under a flow of nitrogen. The vessel was then evacuated and backfilled three times. The resulting mixture was heated at 80 Celsius for 72 hours. The reaction mixture was allowed to cool to room temperature. Celite (15 g) and water (150 mL) were added to the reaction mixture and stirred for 10 min. The mixture was filtered through a bed of Celite (8 g). The reaction vessel and Celite cake were rinsed with Ethyl acetate (150 mL). The layers were separated, and the aqueous layer was washed with Ethyl acetate (3 x 50 mL). The combined EtOAc layers were washed with water (4 x 150 mL) and brine (3 x 150 mL). After drying with sodium sulfate, the Ethyl acetate layer was concentrated on a rotary evaporator to and flash column chromatography was performed in isocratic conditions (10%) MTBE in hexanes . All fractions containing the product were pooled and a solution of HCl in ethyl acetate was added dropwise over 20 min at 0 Celsius. A white solid precipitated out of solution almost immediately. The white solid was vacuum filtered and dried under vacuum to produce 2-(3-fluorophenyl)thiophen-3-amine hydrochloride (536 mg, 56.5 % yield) . ¹H NMR (600 MHz, DMSO) δ 7.69 (dd, *J* = 5.6, 2.5 Hz, 1H), 7.58 – 7.50 (m, 2H), 7.45 (d, *J* = 7.8 Hz, 1H), 7.26 (td, *J* = 8.6, 2.5 Hz, 1H), 7.17 (t, *J* = 5.1 Hz, 1H).

8.4 Synthesis of 2-(4-fluorophenyl)thiophen-3-amine (5):



A 3-necked 25 mL round bottomed flask was evacuated and backfilled with nitrogen. DMF (9 mL) and NMP (1 mL) were added under a flow of nitrogen. Potassium 3-aminothiophene-carboxylate (**2**) (500 mg, 2.76 mmol), 1-bromo-4-fluorobenzene (328 μ L, 3 mmol), tetra-n-butylammonium bromide (133 mg, 0.414 mmol), 1,1'-bis(diphenylphosphino)ferrocene (92 mg, 0.1656 mmol), and palladium(II) chloride (37 mg, 0.206 mmol) were added under a flow of nitrogen. The vessel was then evacuated and backfilled three times. The resulting mixture was heated at 80 Celsius for 72 hours. The reaction mixture was allowed to cool to room temperature. Celite (15 g) and water (150 mL) were added to the reaction mixture and stirred for 10 min. The mixture was filtered through a bed of Celite (8 g). The reaction vessel and Celite cake were rinsed with Ethyl acetate (150 mL). The layers were separated, and the aqueous layer was washed with Ethyl acetate (3 x 50 mL). The combined EtOAc layers were washed with water (4 x 150 mL) and brine (3 x 150 mL). After drying with sodium sulfate, the Ethyl acetate layer was concentrated on a rotary evaporator to and flash column chromatography was performed in isocratic conditions (10%) MTBE in hexanes . All fractions containing the product were pooled and a solution of HCl in ethyl acetate was added dropwise over 20 min at 0 Celsius. A white solid precipitated out of solution almost immediately. The white solid was vacuum filtered and dried under vacuum to produce 2-(4-fluorophenyl)thiophen-3-amine hydrochloride (569 mg, 61 % yield). $^1\text{H NMR}$ (600 MHz, DMSO) δ 7.73 – 7.60 (m, 2H), 7.35 (t, J = 8.8 Hz, 2H), 7.19 (dt, J = 8.9, 4.3 Hz, 1H).

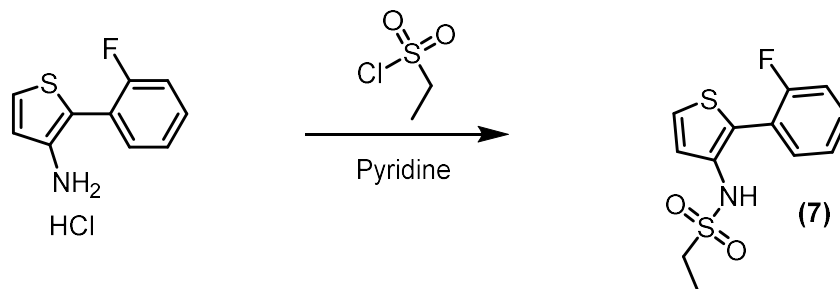
8.5 Synthesis of N-(2-(2-fluorophenyl)thiophen-3-yl)methanesulfonamide (**6**)



2-(2-fluorophenyl)thiophen-3-amine hydrochloride (**3**) (50. mg, 0.22 mmol) was added to a 4 mL 1 dram vial and dissolved in 1 mL pyridine. The flask was cooled to 0 °C in an ice bath before the addition of 2 equivalents (0.264 mmol, 20 μ L) of methanesulfonyl chloride. The bath was allowed to warm up naturally to room temperature and left to stir overnight. Subsequently, the solvent was removed in vacuo. The product was purified by flash column chromatography using a gradient of dichloromethane in hexanes (25 - 100 %) to provide N-(2-(2-fluorophenyl)thiophen-3-yl)methanesulfonamide (57 mg, 0.21 mmol 95% yield) $^1\text{H NMR}$ (600 MHz, DMSO) δ 9.29 (s,

1H), 7.67 (d, $J = 5.4$ Hz, 1H), 7.57 (td, $J = 7.7, 1.8$ Hz, 1H), 7.46 (dddd, $J = 8.6, 7.1, 5.2, 1.8$ Hz, 1H), 7.33 – 7.26 (m, 2H), 7.19 (d, $J = 5.4$ Hz, 1H), 2.89 (s, 3H).

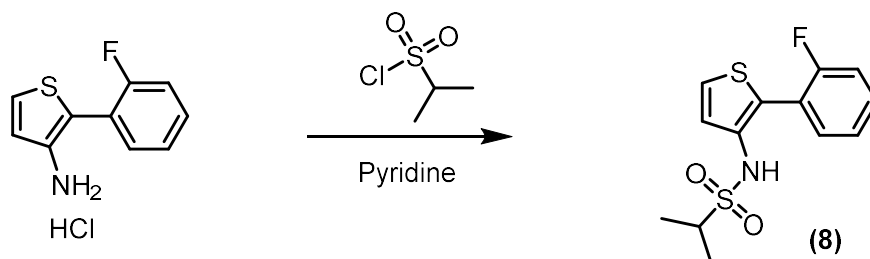
8.6 Synthesis of N-(2-(2-fluorophenyl)thiophen-3-yl)ethanesulfonamide (7)



2-(2-fluorophenyl)thiophen-3-amine hydrochloride (**3**) (50. mg, 0.22 mmol) was added to a 4 mL 1 dram vial and dissolved in 1 mL pyridine. The flask was cooled to 0 °C in an ice bath before the addition of ethanesulfonyl chloride (0.264 mmol, 25 μ L). The bath was allowed to warm up naturally to room temperature and left to stir overnight. Subsequently, the solvent was removed in vacuo. The product was purified by flash column chromatography using a gradient of dichloromethane in hexanes (25 - 100 %) to provide N-(2-(2-fluorophenyl)thiophen-3-yl)ethanesulfonamide (60 mg, 0.21 mmol 95% yield)

^1H NMR (600 MHz, DMSO) δ 9.25 (s, 1H), 7.65 (d, $J = 5.4$ Hz, 1H), 7.57 (td, $J = 7.7, 1.8$ Hz, 1H), 7.46 (dddd, $J = 8.3, 7.2, 5.2, 1.8$ Hz, 1H), 7.34 – 7.25 (m, 2H), 7.15 (d, $J = 5.4$ Hz, 1H), 2.94 (q, $J = 7.3$ Hz, 2H), 1.08 (t, $J = 7.3$ Hz, 3H).

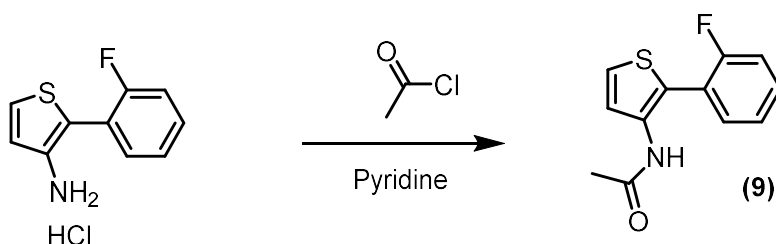
8.7 Synthesis of N-(2-(2-fluorophenyl)thiophen-3-yl)propane-2-sulfonamide (8)



2-(2-fluorophenyl)thiophen-3-amine hydrochloride (**3**) (50. mg, 0.22 mmol) was added to a 4 mL 1 dram vial and dissolved in 1 mL pyridine. The flask was cooled to 0 °C in an ice bath before

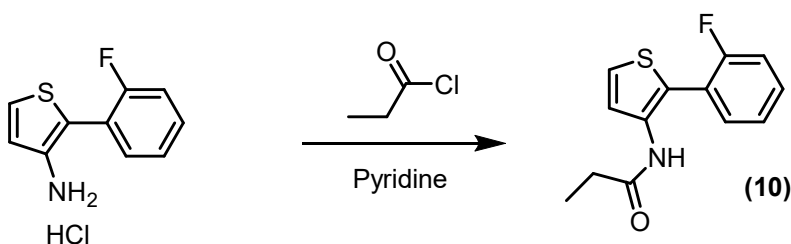
the addition of propane-2-sulfonyl chloride (0.264 mmol, 27 μ L). The bath was allowed to warm up naturally to room temperature and left to stir overnight. Subsequently, the solvent was removed in vacuo. The product was purified by flash column chromatography using a gradient of dichloromethane in hexanes (25 - 100 %) to provide N-(2-(2-fluorophenyl)thiophen-3-yl)propane-2-sulfonamide (43 mg, 0.14 mmol 68 % yield) ^1H NMR (600 MHz, DMSO) δ 9.18 (s, 1H), 7.64 (d, J = 5.4 Hz, 1H), 7.56 (td, J = 7.6, 1.8 Hz, 1H), 7.47 (dddd, J = 8.3, 7.2, 5.3, 1.8 Hz, 1H), 7.34 – 7.24 (m, 2H), 7.14 (d, J = 5.4 Hz, 1H), 3.04 (p, J = 6.8 Hz, 1H), 1.11 (d, J = 6.8 Hz, 6H).

8.8 Synthesis of N-(2-(2-fluorophenyl)thiophen-3-yl)acetamide (9)



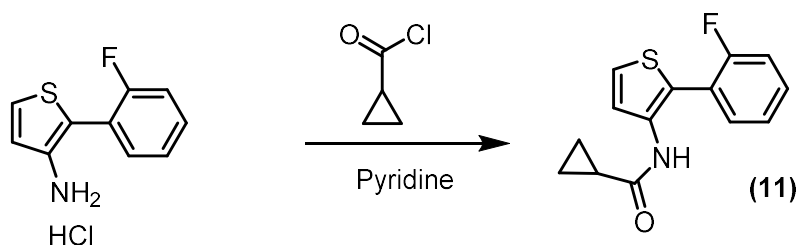
2-(2-fluorophenyl)thiophen-3-amine hydrochloride (**3**) (50. mg, 0.22 mmol) was added to a 4 mL 1 dram vial and dissolved in 1 mL pyridine. The flask was cooled to 0 $^{\circ}\text{C}$ in an ice bath before the addition of acetyl chloride (0.264 mmol, 19 μ L). The bath was allowed to warm up naturally to room temperature and left to stir overnight. Subsequently, the solvent was removed in vacuo. The product was purified by flash column chromatography using a gradient of dichloromethane in hexanes (25 - 100 %) to provide N-(2-(2-fluorophenyl)thiophen-3-yl)acetamide (47 mg, 0.20 mmol 91 % yield) ^1H NMR (600 MHz, DMSO) δ 9.64 (s, 1H), 7.54 (d, J = 5.3 Hz, 1H), 7.49 (td, J = 8.2, 6.3 Hz, 1H), 7.37 – 7.31 (m, 2H), 7.25 (d, J = 5.4 Hz, 1H), 7.22 – 7.16 (m, 1H), 2.01 (s, 3H).

8.9 Synthesis of N-(2-(2-fluorophenyl)thiophen-3-yl)propionamide (10)



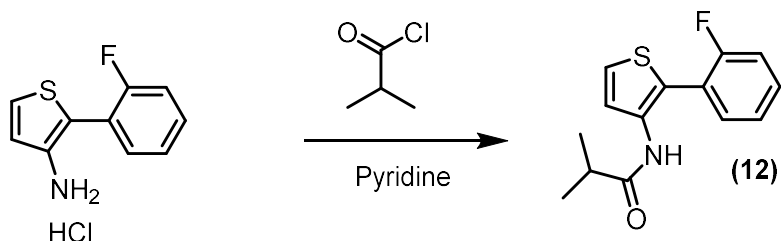
2-(2-fluorophenyl)thiophen-3-amine hydrochloride (**3**) (50. mg, 0.22 mmol) was added to a 4 mL 1 dram vial and dissolved in 1 mL pyridine. The flask was cooled to 0 °C in an ice bath before the addition of propionyl chloride (0.264 mmol, 23 μ L). The bath was allowed to warm up naturally to room temperature and left to stir overnight. Subsequently, the solvent was removed in vacuo. The product was purified by flash column chromatography using a gradient of dichloromethane in hexanes (25 - 100 %) to provide N-(2-(2-fluorophenyl)thiophen-3-yl)acetamide (46 mg, 0.18 mmol, 84 % yield) ^1H NMR (600 MHz, DMSO) δ 9.25 (s, 1H), 7.65 (d, J = 5.4 Hz, 1H), 7.56 (td, J = 7.7, 1.8 Hz, 1H), 7.47 (tdd, J = 7.2, 5.3, 1.8 Hz, 1H), 7.35 – 7.25 (m, 2H), 7.15 (d, J = 5.4 Hz, 1H), 2.94 (q, J = 7.3 Hz, 2H), 1.08 (t, J = 7.3 Hz, 3H).

8.10 Synthesis of N-(2-(2-fluorophenyl)thiophen-3-yl)cyclopropanecarboxamide (**11**)



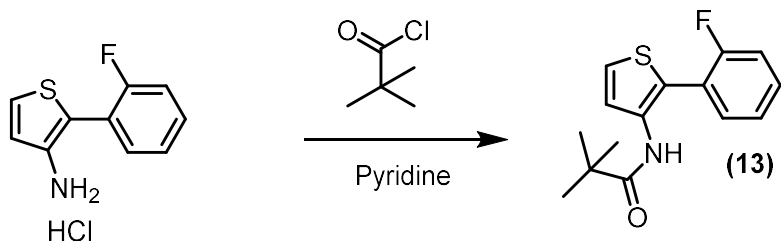
2-(2-fluorophenyl)thiophen-3-amine hydrochloride (**3**) (50. mg, 0.22 mmol) was added to a 4 mL 1 dram vial and dissolved in 1 mL pyridine. The flask was cooled to 0 °C in an ice bath before the addition of Cyclopropanecarbonyl chloride (0.264 mmol, 24 μ L). The bath was allowed to warm up naturally to room temperature and left to stir overnight. Subsequently, the solvent was removed in vacuo. The product was purified by flash column chromatography using a gradient of dichloromethane in hexanes (25 - 100 %) to provide N-(2-(2-fluorophenyl)thiophen-3-yl)acetamide (39 mg, 0.15 mmol 68 % yield) ^1H NMR (600 MHz, DMSO) δ 9.75 (s, 1H), 7.59 (d, J = 5.4 Hz, 1H), 7.49 – 7.42 (m, 2H), 7.39 (d, J = 5.4 Hz, 1H), 7.35 – 7.26 (m, 2H), 1.83 – 1.76 (m, 1H), 0.79 – 0.69 (m, 4H).

8.11 Synthesis of N-(2-(2-fluorophenyl)thiophen-3-yl)isobutyramide (12)



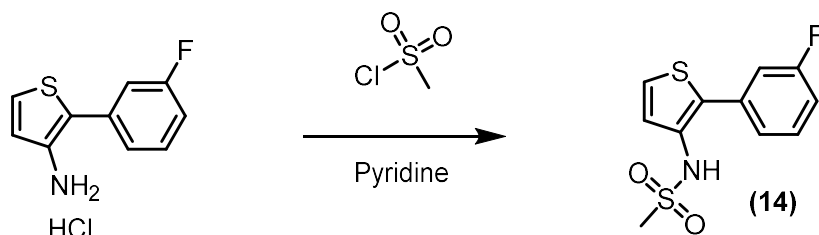
2-(2-fluorophenyl)thiophen-3-amine hydrochloride (**3**) (50. mg, 0.22 mmol) was added to a 4 mL 1 dram vial and dissolved in 1 mL pyridine. The flask was cooled to 0 °C in an ice bath before the addition of isobutyryl chloride (0.264 mmol, 27 μ L). The bath was allowed to warm up naturally to room temperature and left to stir overnight. Subsequently, the solvent was removed in vacuo. The product was purified by flash column chromatography using a gradient of dichloromethane in hexanes (25 - 100 %) to provide N-(2-(2-fluorophenyl)thiophen-3-yl)acetamide (45 mg, 0.17 mmol 77 % yield) ^1H NMR (600 MHz, DMSO) δ 7.60 (d, J = 5.4 Hz, 1H), 7.48 – 7.39 (m, 2H), 7.34 (d, J = 5.4 Hz, 1H), 7.33 – 7.24 (m, 2H), 2.56 (h, J = 6.9 Hz, 1H), 1.03 (d, J = 6.9 Hz, 6H).

8.12 Synthesis of N-(2-(2-fluorophenyl)thiophen-3-yl)pivalamide (13)



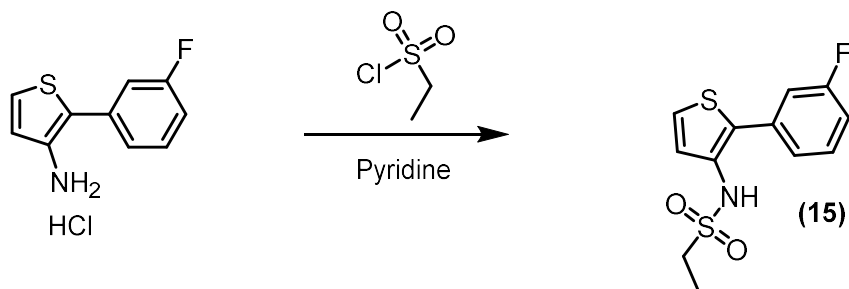
2-(2-fluorophenyl)thiophen-3-amine hydrochloride (**3**) (50. mg, 0.22 mmol) was added to a 4 mL 1 dram vial and dissolved in 1 mL pyridine. The flask was cooled to 0 °C in an ice bath before the addition of pivaloyl chloride (0.264 mmol, 32 μ L). The bath was allowed to warm up naturally to room temperature and left to stir overnight. Subsequently, the solvent was removed in vacuo. The product was purified by flash column chromatography using a gradient of dichloromethane in hexanes (25 - 100 %) to provide N-(2-(2-fluorophenyl)thiophen-3-yl)acetamide (32 mg, 0.12 mmol 53 % yield) ^1H NMR (600 MHz, DMSO) δ 7.60 (d, J = 5.4 Hz, 1H), 7.48 – 7.39 (m, 2H), 7.34 (d, J = 5.4 Hz, 1H), 7.33 – 7.24 (m, 2H), 1.13 (s, 9H).

8.13 Synthesis of N-(2-(3-fluorophenyl)thiophen-3-yl)methanesulfonamide (14)



2-(3-fluorophenyl)thiophen-3-amine hydrochloride (**4**) (50. mg, 0.22 mmol) was added to a 4 mL 1 dram vial and dissolved in 1 mL pyridine. The flask was cooled to 0 °C in an ice bath before the addition of 2 equivalents (0.264 mmol, 20 μ L) of methanesulfonyl chloride. The bath was allowed to warm up naturally to room temperature and left to stir overnight. Subsequently, the solvent was removed in vacuo. The product was purified by flash column chromatography using a gradient of dichloromethane in hexanes (25 - 100 %) to provide N-(2-(3-fluorophenyl)thiophen-3-yl)methanesulfonamide (57 mg, 0.21 mmol 95% yield) ^1H NMR (600 MHz, DMSO) δ 9.34 (s, 1H), 7.62 (d, J = 5.4 Hz, 1H), 7.55 (d, J = 10.8 Hz, 1H), 7.53 – 7.42 (m, 2H), 7.22 (t, J = 7.4 Hz, 1H), 7.16 (d, J = 5.4 Hz, 1H), 2.91 (s, 3H).

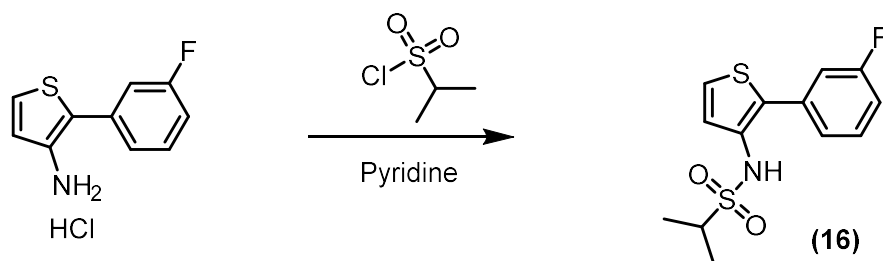
8.14 Synthesis of N-(2-(3-fluorophenyl)thiophen-3-yl)ethanesulfonamide (15)



2-(3-fluorophenyl)thiophen-3-amine hydrochloride (**4**) (50. mg, 0.22 mmol) was added to a 4 mL 1 dram vial and dissolved in 1 mL pyridine. The flask was cooled to 0 °C in an ice bath before

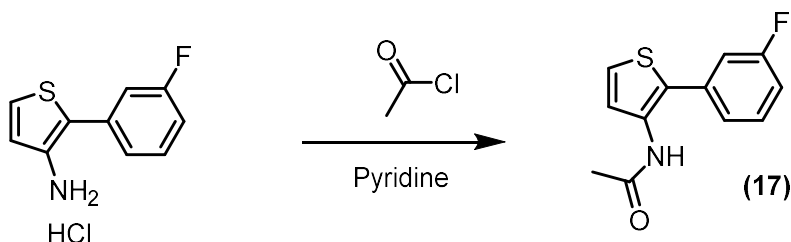
the addition of ethanesulfonyl chloride (0.264 mmol, 25 μ L). The bath was allowed to warm up naturally to room temperature and left to stir overnight. Subsequently, the solvent was removed in vacuo. The product was purified by flash column chromatography using a gradient of dichloromethane in hexanes (25 - 100 %) to provide N-(2-(3-fluorophenyl)thiophen-3-yl)ethanesulfonamide (60 mg, 0.21 mmol 95% yield) ^1H NMR (600 MHz, DMSO) δ 9.31 (s, 1H), 7.60 (d, J = 5.4 Hz, 1H), 7.54 (dt, J = 10.5, 2.1 Hz, 1H), 7.50 (td, J = 8.0, 6.1 Hz, 1H), 7.45 (dt, J = 7.7, 1.3 Hz, 1H), 7.25 – 7.18 (m, 1H), 7.11 (d, J = 5.4 Hz, 1H), 2.96 (q, J = 7.3 Hz, 2H), 1.11 (t, J = 7.3 Hz, 3H).

8.15 Synthesis of N-(2-(3-fluorophenyl)thiophen-3-yl)propane-2-sulfonamide (16)



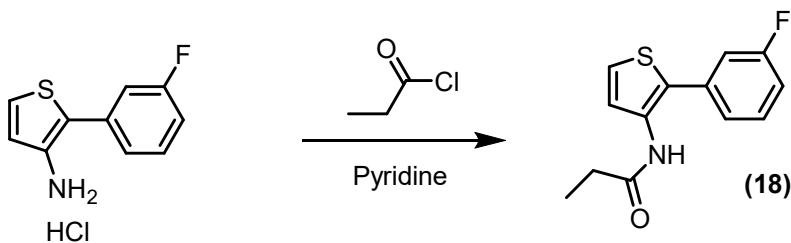
2-(3-fluorophenyl)thiophen-3-amine hydrochloride (**4**) (50. mg, 0.22 mmol) was added to a 4 mL 1 dram vial and dissolved in 1 mL pyridine. The flask was cooled to 0 $^{\circ}$ C in an ice bath before the addition of propane-2-esulfonyl chloride (0.264 mmol, 27 μ L). The bath was allowed to warm up naturally to room temperature and left to stir overnight. Subsequently, the solvent was removed in vacuo. The product was purified by flash column chromatography using a gradient of dichloromethane in hexanes (25 - 100 %) to provide N-(2-(3-fluorophenyl)thiophen-3-yl)propane-2-sulfonamide (43 mg, 0.14 mmol 68 % yield) ^1H NMR (600 MHz, DMSO) δ 9.18 (s, 1H), 7.64 (d, J = 5.4 Hz, 1H), 7.56 (td, J = 7.6, 1.8 Hz, 1H), 7.47 (dddd, J = 8.3, 7.2, 5.3, 1.8 Hz, 1H), 7.34 – 7.24 (m, 2H), 7.14 (d, J = 5.4 Hz, 1H), 3.04 (p, J = 6.8 Hz, 1H), 1.11 (d, J = 6.8 Hz, 6H).

8.16 Synthesis of N-(2-(3-fluorophenyl)thiophen-3-yl)acetamide (17)



2-(3-fluorophenyl)thiophen-3-amine hydrochloride (**4**) (50. mg, 0.22 mmol) was added to a 4 mL 1 dram vial and dissolved in 1 mL pyridine. The flask was cooled to 0 °C in an ice bath before the addition of acetyl chloride (0.264 mmol, 19 μ L). The bath was allowed to warm up naturally to room temperature and left to stir overnight. Subsequently, the solvent was removed in vacuo. The product was purified by flash column chromatography using a gradient of dichloromethane in hexanes (25 - 100 %) to provide N-(2-(3-fluorophenyl)thiophen-3-yl)acetamide (47 mg, 0.20 mmol 91 % yield) ^1H NMR (600 MHz, DMSO) δ 9.64 (s, 1H), 7.54 (d, J = 5.3 Hz, 1H), 7.49 (td, J = 8.2, 6.3 Hz, 1H), 7.37 – 7.31 (m, 2H), 7.25 (d, J = 5.4 Hz, 1H), 7.22 – 7.16 (m, 1H), 2.01 (s, 3H).

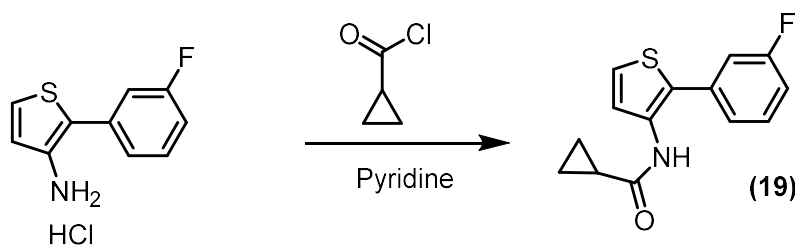
8.17 Synthesis of N-(2-(3-fluorophenyl)thiophen-3-yl)propionamide (18)



2-(3-fluorophenyl)thiophen-3-amine hydrochloride (**4**) (50. mg, 0.22 mmol) was added to a 4 mL 1 dram vial and dissolved in 1 mL pyridine. The flask was cooled to 0 °C in an ice bath before the addition of propionyl chloride (0.264 mmol, 23 μ L). The bath was allowed to warm up naturally to room temperature and left to stir overnight. Subsequently, the solvent was removed in vacuo. The product was purified by flash column chromatography using a gradient of dichloromethane in hexanes (25 - 100 %) to provide N-(2-(3-fluorophenyl)thiophen-3-

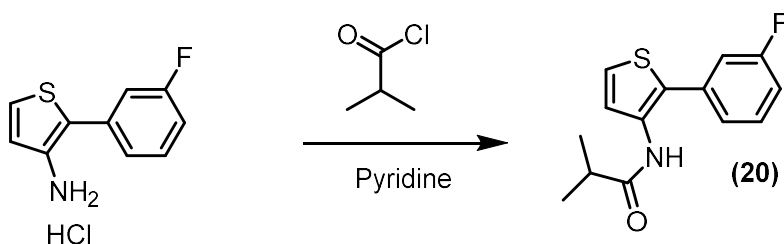
yl)acetamide (46 mg, 0.18 mmol, 84 % yield) ^1H NMR (600 MHz, DMSO) δ 9.57 (s, 1H), 7.54 (d, $J = 5.4$ Hz, 1H), 7.49 (td, $J = 8.1, 6.3$ Hz, 1H), 7.36 – 7.30 (m, 2H), 7.24 (d, $J = 5.3$ Hz, 1H), 7.21 – 7.16 (m, 1H), 2.29 (q, $J = 7.6$ Hz, 2H), 1.07 (t, $J = 7.6$ Hz, 3H).

8.18 Synthesis of N-(2-(3-fluorophenyl)thiophen-3-yl)cyclopropanecarboxamide (19)



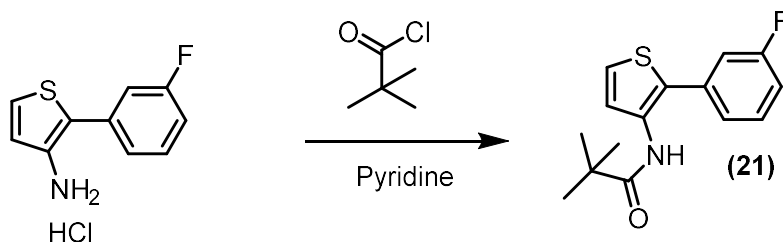
2-(3-fluorophenyl)thiophen-3-amine hydrochloride (**4**) (50. mg, 0.22 mmol) was added to a 4 mL 1 dram vial and dissolved in 1 mL pyridine. The flask was cooled to 0 °C in an ice bath before the addition of Cyclopropanecarbonyl chloride (0.264 mmol, 24 μL). The bath was allowed to warm up naturally to room temperature and left to stir overnight. Subsequently, the solvent was removed in vacuo. The product was purified by flash column chromatography using a gradient of dichloromethane in hexanes (25 - 100 %) to provide N-(2-(3-fluorophenyl)thiophen-3-yl)acetamide (39 mg, 0.15 mmol 68 % yield) ^1H NMR (600 MHz, DMSO) δ 7.54 (d, $J = 5.4$ Hz, 1H), 7.50 (td, $J = 8.1, 6.2$ Hz, 1H), 7.38 – 7.31 (m, 2H), 7.24 (d, $J = 5.4$ Hz, 1H), 7.19 (ddd, $J = 10.4, 8.2, 2.7$ Hz, 1H), 1.82 (p, $J = 6.3$ Hz, 1H), 0.77 (d, $J = 6.2$ Hz, 4H).

8.19 Synthesis of N-(2-(3-fluorophenyl)thiophen-3-yl)isobutyramide (20)



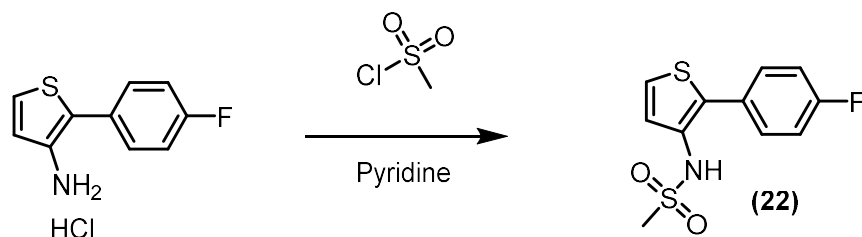
2-(3-fluorophenyl)thiophen-3-amine hydrochloride (**4**) (50. mg, 0.22 mmol) was added to a 4 mL 1 dram vial and dissolved in 1 mL pyridine. The flask was cooled to 0 °C in an ice bath before the addition of isobutyryl chloride (0.264 mmol, 27 μ L). The bath was allowed to warm up naturally to room temperature and left to stir overnight. Subsequently, the solvent was removed in vacuo. The product was purified by flash column chromatography using a gradient of dichloromethane in hexanes (25 - 100 %) to provide N-(2-(3-fluorophenyl)thiophen-3-yl)acetamide (45 mg, 0.17 mmol 77 % yield) ^1H NMR (600 MHz, DMSO) δ 9.53 (s, 1H), 7.55 (d, J = 5.3 Hz, 1H), 7.49 (td, J = 8.1, 6.2 Hz, 1H), 7.35 – 7.29 (m, 2H), 7.19 (d, J = 5.4 Hz, 1H), 2.64 – 2.55 (m, 1H), 1.08 (d, J = 6.8 Hz, 6H).

8.20 Synthesis of N-(2-(3-fluorophenyl)thiophen-3-yl)pivalamide (**21**)



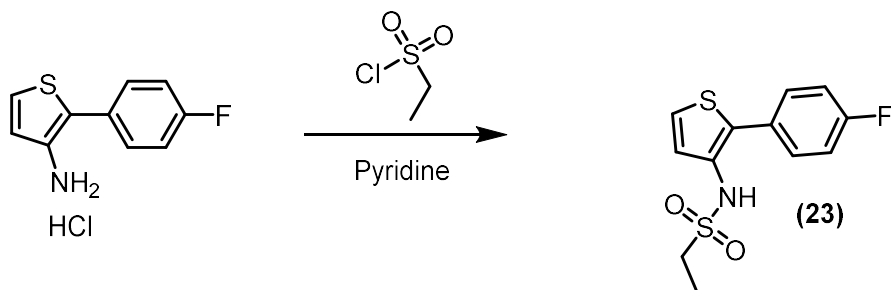
2-(3-fluorophenyl)thiophen-3-amine hydrochloride (**4**) (50. mg, 0.22 mmol) was added to a 4 mL 1 dram vial and dissolved in 1 mL pyridine. The flask was cooled to 0 °C in an ice bath before the addition of pivaloyl chloride (0.264 mmol, 32 μ L). The bath was allowed to warm up naturally to room temperature and left to stir overnight. Subsequently, the solvent was removed in vacuo. The product was purified by flash column chromatography using a gradient of dichloromethane in hexanes (25 - 100 %) to provide N-(2-(3-fluorophenyl)thiophen-3-yl)acetamide (32 mg, 0.12 mmol 53 % yield) ^1H NMR (600 MHz, DMSO) δ 9.53 (s, 1H), 7.55 (d, J = 5.3 Hz, 1H), 7.49 (td, J = 8.1, 6.2 Hz, 1H), 7.35 – 7.29 (m, 2H), 7.19 (d, J = 5.4 Hz, 1H), 1.12 (s, 9H).

8.21 Synthesis of N-(2-(4-fluorophenyl)thiophen-3-yl)methanesulfonamide (22)



2-(4-fluorophenyl)thiophen-3-amine hydrochloride (**5**) (50. mg, 0.22 mmol) was added to a 4 mL 1 dram vial and dissolved in 1 mL pyridine. The flask was cooled to 0 °C in an ice bath before the addition of 2 equivalents (0.264 mmol, 20 μ L) of methanesulfonyl chloride. The bath was allowed to warm up naturally to room temperature and left to stir overnight. Subsequently, the solvent was removed in vacuo. The product was purified by flash column chromatography using a gradient of dichloromethane in hexanes (25 - 100 %) to provide N-(2-(4-fluorophenyl)thiophen-3-yl)methanesulfonamide (57 mg, 0.21 mmol 95% yield) ^1H NMR (600 MHz, DMSO) δ 9.26 (s, 1H), 7.69 (ddd, J = 8.7, 5.5, 2.7 Hz, 2H), 7.56 (d, J = 5.4 Hz, 1H), 7.33 – 7.26 (m, 2H), 7.14 (d, J = 5.4 Hz, 1H), 2.88 (s, 3H).

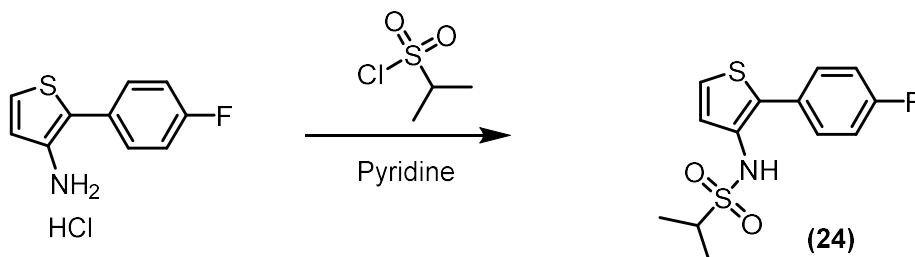
8.22 Synthesis of N-(2-(4-fluorophenyl)thiophen-3-yl)ethanesulfonamide (23)



2-(4-fluorophenyl)thiophen-3-amine hydrochloride (**5**) (50. mg, 0.22 mmol) was added to a 4 mL 1 dram vial and dissolved in 1 mL pyridine. The flask was cooled to 0 °C in an ice bath before the addition of ethanesulfonyl chloride (0.264 mmol, 25 μ L). The bath was allowed to warm up naturally to room temperature and left to stir overnight. Subsequently, the solvent was removed in vacuo. The product was purified by flash column chromatography using a gradient of dichloromethane in hexanes (25 - 100 %) to provide N-(2-(4-fluorophenyl)thiophen-3-yl)ethanesulfonamide (60 mg, 0.21 mmol 95% yield) ^1H NMR (600 MHz, DMSO) δ 9.26 (s, 1H),

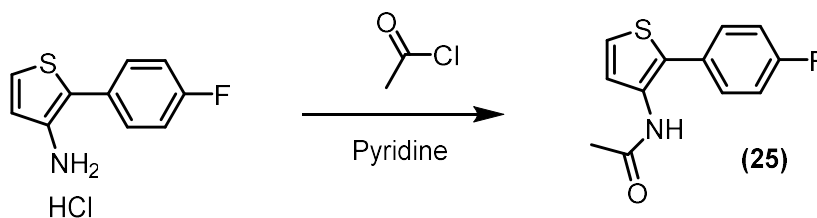
7.69 (ddd, $J = 8.7, 5.5, 2.7$ Hz, 2H), 7.56 (d, $J = 5.4$ Hz, 1H), 7.33 – 7.26 (m, 2H), 7.14 (d, $J = 5.4$ Hz, 1H), 2.88 (m, 2H), 1.10 (t, $J = 6.5$ Hz, 3H)

8.23 Synthesis of N-(2-(4-fluorophenyl)thiophen-3-yl)propane-2-sulfonamide (24)



2-(4-fluorophenyl)thiophen-3-amine hydrochloride (**5**) (50. mg, 0.22 mmol) was added to a 4 mL 1 dram vial and dissolved in 1 mL pyridine. The flask was cooled to 0 °C in an ice bath before the addition of propane-2-sulfonyl chloride (0.264 mmol, 27 μ L). The bath was allowed to warm up naturally to room temperature and left to stir overnight. Subsequently, the solvent was removed in vacuo. The product was purified by flash column chromatography using a gradient of dichloromethane in hexanes (25 - 100 %) to provide N-(2-(4-fluorophenyl)thiophen-3-yl)propane-2-sulfonamide (43 mg, 0.14 mmol 68 % yield)

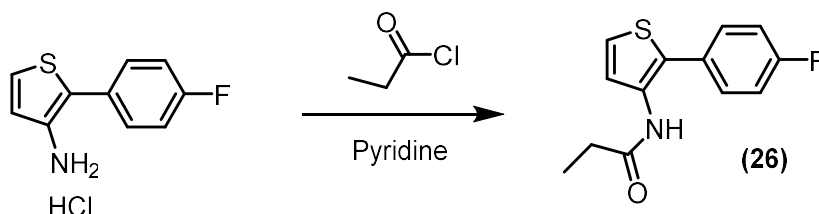
8.24 Synthesis of N-(2-(4-fluorophenyl)thiophen-3-yl)acetamide (25)



2-(4-fluorophenyl)thiophen-3-amine hydrochloride (**5**) (50. mg, 0.22 mmol) was added to a 4 mL 1 dram vial and dissolved in 1 mL pyridine. The flask was cooled to 0 °C in an ice bath before the addition of acetyl chloride (0.264 mmol, 19 μ L). The bath was allowed to warm up naturally to room temperature and left to stir overnight. Subsequently, the solvent was removed in vacuo. The product was purified by flash column chromatography using a gradient of dichloromethane

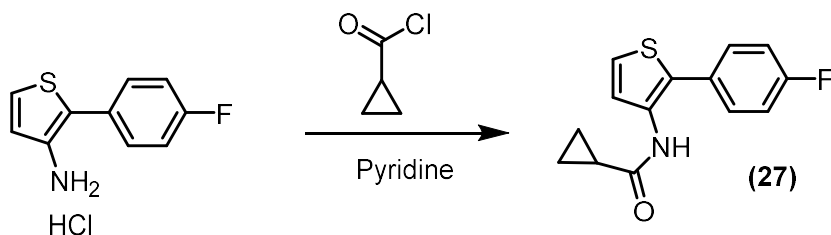
in hexanes (25 - 100 %) to provide N-(2-(4-fluorophenyl)thiophen-3-yl)acetamide (47 mg, 0.20 mmol 91 % yield) ¹H NMR (600 MHz, DMSO) δ 9.55 (s, 1H), 7.57 – 7.50 (m, 2H), 7.49 (d, *J* = 5.4 Hz, 1H), 7.29 (dd, *J* = 9.8, 7.7 Hz, 2H), 7.22 (d, *J* = 5.3 Hz, 1H), 1.99 (s, 3H).

8.25 Synthesis of N-(2-(4-fluorophenyl)thiophen-3-yl)propionamide (26)



2-(4-fluorophenyl)thiophen-3-amine hydrochloride (**5**) (50. mg, 0.22 mmol) was added to a 4 mL 1 dram vial and dissolved in 1 mL pyridine. The flask was cooled to 0 °C in an ice bath before the addition of acetyl chloride (0.264 mmol, 19 μL). The bath was allowed to warm up naturally to room temperature and left to stir overnight. Subsequently, the solvent was removed in vacuo. The product was purified by flash column chromatography using a gradient of dichloromethane in hexanes (25 - 100 %) to provide N-(2-(4-fluorophenyl)thiophen-3-yl)acetamide (47 mg, 0.20 mmol 91 % yield) ¹H NMR (600 MHz, DMSO) δ 7.71 – 7.57 (m, 2H), 7.32 (t, *J* = 8.8 Hz, 2H), 7.23 (dt, *J* = 8.9, 4.3 Hz, 1H). 2.30 (q, *J* = 7.6 Hz, 2H), 1.05 (t, *J* = 7.6 Hz, 3H).

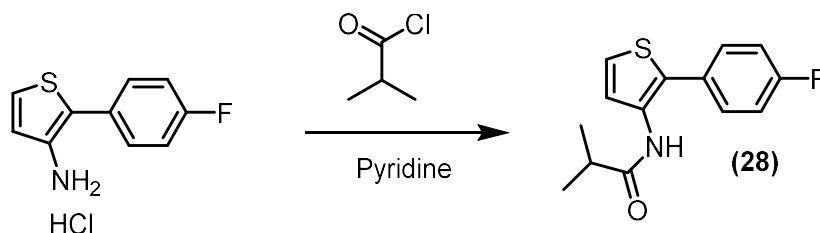
8.26 Synthesis of N-(2-(4-fluorophenyl)thiophen-3-yl)cyclopropanecarboxamide (27)



2-(4-fluorophenyl)thiophen-3-amine hydrochloride (**5**) (50. mg, 0.22 mmol) was added to a 4 mL 1 dram vial and dissolved in 1 mL pyridine. The flask was cooled to 0 °C in an ice bath before the addition of Cyclopropanecarbonyl chloride (0.264 mmol, 24 μL). The bath was allowed to warm up naturally to room temperature and left to stir overnight. Subsequently, the solvent was removed in vacuo. The product was purified by flash column chromatography using a gradient of dichloromethane in hexanes (25 - 100 %) to provide N-(2-(4-fluorophenyl)thiophen-3-

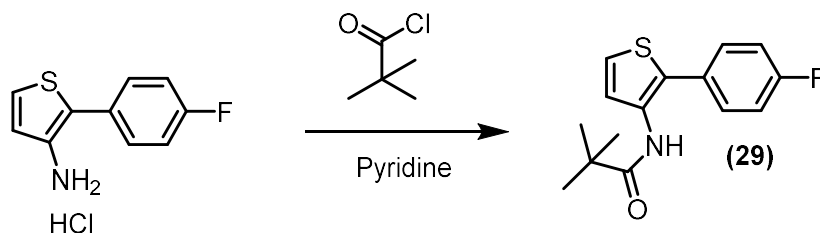
yl)acetamide (39 mg, 0.15 mmol 68 % yield) ^1H NMR (600 MHz, DMSO) δ 7.75 – 7.62 (m, 2H), 7.34 (t, J = 8.8 Hz, 2H), 7.20 (dt, J = 8.8, 4.3 Hz, 1H). 1.81 (p, J = 6.3 Hz, 1H), 0.75 (d, J = 6.2 Hz, 4H).

8.27 Synthesis of N-(2-(4-fluorophenyl)thiophen-3-yl)isobutyramide (28)



2-(4-fluorophenyl)thiophen-3-amine hydrochloride (**5**) (50. mg, 0.22 mmol) was added to a 4 mL 1 dram vial and dissolved in 1 mL pyridine. The flask was cooled to 0 °C in an ice bath before the addition of isobutyryl chloride (0.264 mmol, 27 μL). The bath was allowed to warm up naturally to room temperature and left to stir overnight. Subsequently, the solvent was removed in vacuo. The product was purified by flash column chromatography using a gradient of dichloromethane in hexanes (25 - 100 %) to provide N-(2-(4-fluorophenyl)thiophen-3-yl)acetamide (45 mg, 0.17 mmol 77 % yield) ^1H NMR (600 MHz, DMSO) δ 7.73 – 7.60 (m, 2H), 7.35 (t, J = 8.8 Hz, 2H), 7.19 (dt, J = 8.9, 4.3 Hz, 1H). 2.54 (h, J = 6.9 Hz, 1H), 1.05 (d, J = 6.9 Hz, 6H)

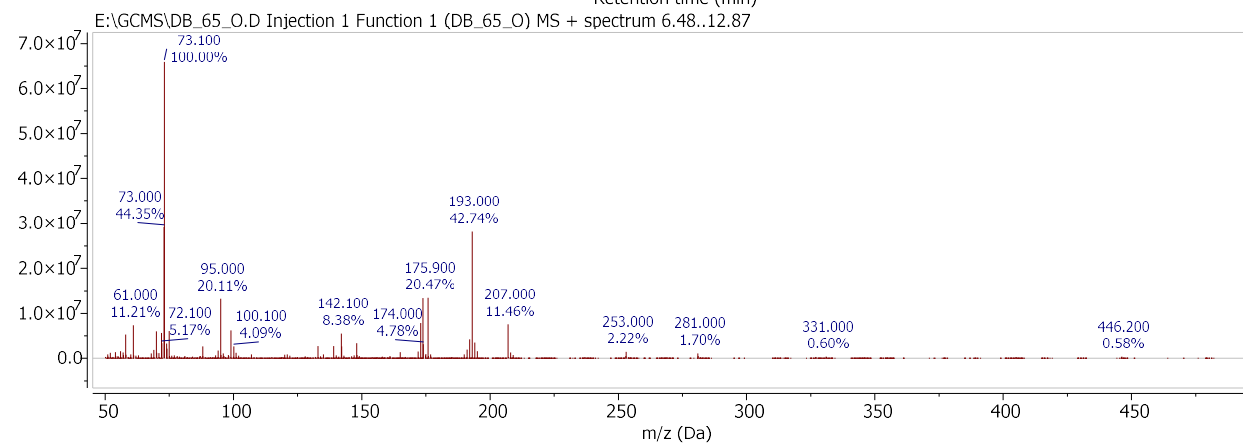
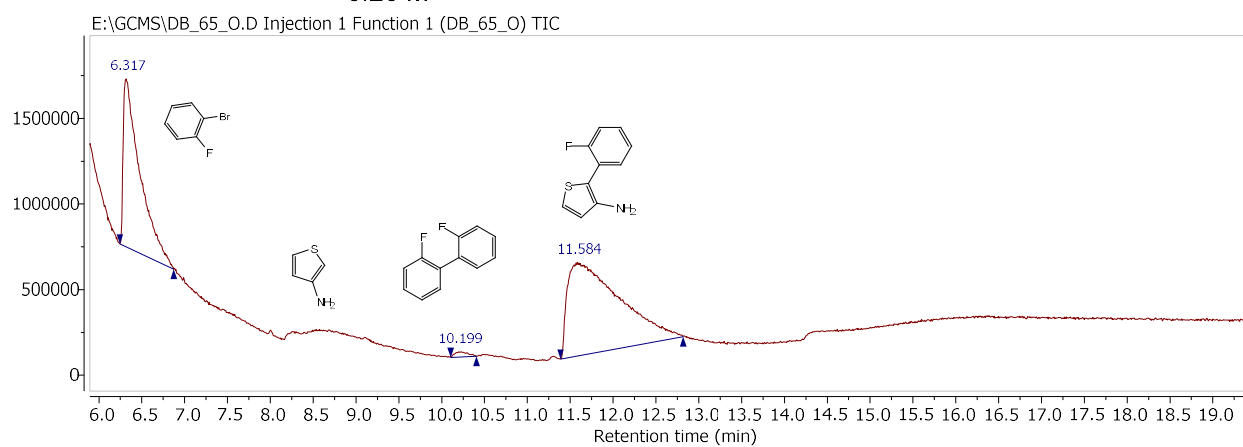
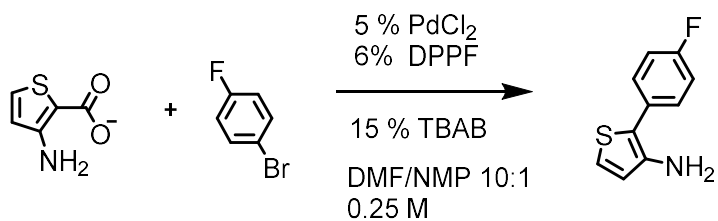
8.28 Synthesis of N-(2-(4-fluorophenyl)thiophen-3-yl)pivalamide (29)



2-(4-fluorophenyl)thiophen-3-amine hydrochloride (**5**) (50. mg, 0.22 mmol) was added to a 4 mL 1 dram vial and dissolved in 1 mL pyridine. The flask was cooled to 0 °C in an ice bath before the addition of pivaloyl chloride (0.264 mmol, 32 μL). The bath was allowed to warm up naturally to room temperature and left to stir overnight. Subsequently, the solvent was removed in vacuo. The product was purified by flash column chromatography using a gradient of dichloromethane in hexanes (25 - 100 %) to provide N-(2-(2-fluorophenyl)thiophen-3-yl)acetamide (32 mg, 0.12

mmol 53 % yield) ¹H NMR (600 MHz, DMSO) δ 7.70 – 7.58 (m, 2H), 7.32 (t, *J* = 8.8 Hz, 2H), 7.21 (dt, *J* = 8.9, 4.3 Hz, 1H), 1.08 (s, 9H)

GC-MS of Para coupling reaction



GC-MS of Ortho coupling reaction

